Biointerface Research in Applied Chemistry
Open-Access Journal (ISSN: 2069-5837)

Review
Volume 13, Issue 5, 2023, 457
https://doi.org/10.33263/BRIAC135.457

Applications of Graphene and Graphene Oxide as Versatile Sensors: A Brief Review

Reshmi Bose [1], Abdullah K. Alanazi [2], Soumalya Bhowmik [3], Somenath Garai [4], Manas Roy [5], Bholanath Pakhira [6,*], Tanay Pramanik [1,*]

1 Department of Chemistry, University of Engineering and Management, University Area, Action Area III, B/5, Newtown, Kolkata-700160, India
2 Department of Chemistry, College of Science, Taif University, P.O. Box 11099, Taif 21944, Saudi Arabia
3 Centre for Nanotechnology, Indian Institute of Technology Guwahati, Guwahati - 781039, Assam, India
4 Department of Chemistry, Institute of Science, Banaras Hindu University, Varanasi-221005, India
5 Department of Chemistry, National Institute of Technology, Agartala, Barjala, Jirania, Tripura-799046, India
6 Department of Chemistry, Sister Nibedita Govt. General Degree College for Girls, Hatings House, Alipore, Kolkata-700027, India
* Correspondence:pakhirabhola@gmail.com (B.P); tanay.pramanik@gmail.com (T.P);

Scopus Author ID 55917884600
Received: 10.09.2022; Accepted: 6.11.2022; Published: 24.12.2022

Abstract: Graphene is one of the well-known allotropes of carbon and is regarded among the most significant substances of the modern era, having substantially influenced every field of research and now entering the commercial sector. It has earned popularity among researchers owing to some of its special qualities, such as excellent thermal and electrical conductivity. Thus it can be used to make electrical or strain sensors to sense toxic gasses. After the oxidation of graphene through different processes, graphene oxide is formed. As a direct consequence of the existence of oxygenated functional groups, they can also act as gas sensors, biosensors, and electrochemical sensors. This mini-review ruminates the respective implications of graphene and GO as electrical, electrochemical strain, various gas sensors, surface stress sensors, selectivity, and efficiency, along with their advantages and limitations.

Keywords: Graphene; Graphene Oxide; Electrical Sensors, Electrochemical Sensors; Gas Sensors; Bio Sensors

1. Introduction

The advancement of nanotechnology opens a new door for material-based nanoscience, providing many exciting opportunities in biotechnological development due to their special structure, components, and properties[1]. This particular branch of science establishes the real evidence for the statement of Leonardo da Vinci who remarked once, “Where nature finishes producing its species, man begins, using natural things and with the help of this nature, to create an infinity of species.”

In nanotechnology, graphene is one of the nanomaterials that has received the most attention and research[2]. Researchers find a keen desire for graphene and its derivatives, and in the past 40 years, several studies and discussions have been dedicated to the topic. [3–8]. Experimentally it has been found that a very large 2D theoretical area (2630 m^2g^{-1})[9–11], excellent intrinsic mobility (200000 $cm^2V^{-1}s$)[12,13], and superb Young’s Modulus (1.0 TPa)[14] have been shown by graphene. Furthermore, as a result of its high thermal

conductivity, graphene can dissipate heat at a rate of roughly 5000$Wm^{-1}K^{-1}$[15,16]. Since it has a high thermal and electrical conductivity, the material is appropriate for transparent conductive electrodes [17].

Graphene oxide can be prepared via the "modified Hummers method"[18–21], but the conductivity of GO is very lower, nearly insulating in nature. The most interesting feature of GO is that the monolayer consists of six member carbon units with sp2 and sp3 carbons, and each layer is easily dishtinguishable[22]. It also consists of a large basal plane with various functional groups (oxygen-containing) where hydroxyl (-OH) and epoxide (-O-)groups are present on both sides of the plane, and carbonyl (=O) and carboxyl (-COOH) groups are present at the plane's wingtip[23–25]. During oxidation, these hydroxyl groups are converted to the epoxide groups, which is attribute to the defect in the electronic structure that leads to GO insulator properties [26]. These defective structures of GO limit the application in device physics, but for chemists, it grows the interest due to the possibility of forming heterogeneous structures [27].

Both graphene and graphene oxide shows numerous applications in many fields like nanocarriers for drug delivery, applications for producing anti-cancer drugs and photothermal therapy for cancer[28–30], a huge application in biofunctionalization, and applications in biotechnology [31–34], in producing Graphene-Polymer Nanocomposites, they can also be used as biosensors [10,35–37]. Functionalized graphene is often used in sensors for measuring electrochemical, strain, and electrical characteristics[38,39]. Graphene offers special characteristics that make it ideal for certain applications. Compared to more conventional sensing materials, it generates less electrical noise and has fewer crystal defects. It is used as a sensor for detecting dangerous compounds such as hydrazine. It can also be used to find specific molecules like adenine dinucleotide, and hemoglobin and biomolecules like ascorbic acid, uric acid, and others. Pure graphene is mixed with other elements, such as platinum(Pt) and TiO_2, to create nano-composites, and it is being used to improve the sensor's sensitivity and detecting capabilities [40]. When a gas is introduced into low-concentration tubes and then forced to flow over the graphene surface, its concentration of charges changes immediately. Graphene's resistance and conductivity are both affected by the concentration of its charges[40]. Understanding the characteristics of gas molecules is made easier with the help of the values. Chemical sensors (graphene-based) may be produced at a low cost by employing acrylic plastic as a substrate. Eliminating the need for expensive processes like e-beam lithography also speeds up manufacturing and saves money.

Furthermore, an electrochemical sensor (graphene-based) with a dual intake and analyte gas channel has a very quick switching time. Wearable graphene chemical sensor performs at typical air pressure and ambient temperature. Graphene's unique link between mechanical and electrical characteristics has also aided its usage in strain sensing [2].

The present review involves a brief understanding of the synthesis approach of graphene and graphene oxide and their promising applicability as biosensors, electrochemical sensors, and gas sensors. The review concludes with a discussion of graphene and graphene oxide-based sensor-related issues from various future perspectives and technological viewpoints.

2. Synthesis of Graphene Oxide

The research community has utilized numerous synthetic routes to tune the physicochemical properties of graphene. By adjusting the reaction conditions, substrates, and

other factors, a variety of functionalized graphene derivatives have been synthesized—scientist B.C. Brodie found the first graphene-related compounds in 1859 when he saw the brilliant yellow color resulting from the oxidation of the powder form of graphite using a slurry of 1:3 fuming HNO_3 and $KClO_3$. He designated the element "Graphon" at the time. By oxidizing graphite powder in the presence of a potent oxidizing agent (a mixture of $KMnO_4$ and $KClO_3$ in a concentrated H_2SO_4 medium), Prof. H. P. Bohem discovered black, tiny (thin 3.7A^o) graphite lamella almost a century later[3,41]. In previous years, several processes, including the mechanical exfoliation process, chemical method, and chemical vapor deposition (CVD) system, were established to produce graphene and graphene oxide [42]. The Manchester group described using cohesive tape to separate small graphene layers from graphite sheets[43]. Utilizing the vacuum graphitization method, graphene's epitaxial growth was developed after the thermal breakdown of SiC at a temperature of 10,00 °C [44]. On the transition metal substrate, graphene was produced using the CVD process under extreme vacuum and elevated heat conditions. This method involved heating vaporized hydrocarbon material to a temperature of 800 °C in order to produce C-atoms, which then underwent nucleation and grew to form graphene on the metal surface. Bottom-up technology has many advantages, such as creating pristine graphene layers, fewer defects, and quite well-defined methods. However, it cannot be synthesized at low temperatures; rather, it requires extremely high temperatures, making bulk manufacturing difficult and costly. The bottom-up process is widely used for graphene manufacturing due to its ability to control atomic size, shape, configurational stability, and edge structure[45,46]. Hummer's scheme and modified Hummer's strategy are currently the most commonly used techniques for GO production [47,48]. Hummer's method involves the oxidation of graphite powder with a conc. acid mixture of H_2SO_4 and HNO_3, followed by additional oxidation with KMnO4. H_2O_2 was used to neutralize the excess $KMnO_4$ in the reaction medium. When GO is created, an intricate process is required to get rid of the unutilized acid and inorganic ions from the reaction mixture. A modified Hummer's approach was used to synthesize GO for better performance in the procedure's yield, characteristics, and recompenses. In modified Hummer's technique, H_2SO_4/H_3PO_4 was used instead of a mixture of H_2SO_4 and 1.5 g $NaNO_3$ for 3 g of graphite powder, and the yield was four times that of Hummer's method[9]. One of the benefits of this process is that no harmful gases like NOx are made as a result of this process.

Figure 1 summarizes GO's preparation and applicability toward gas sensing [49].

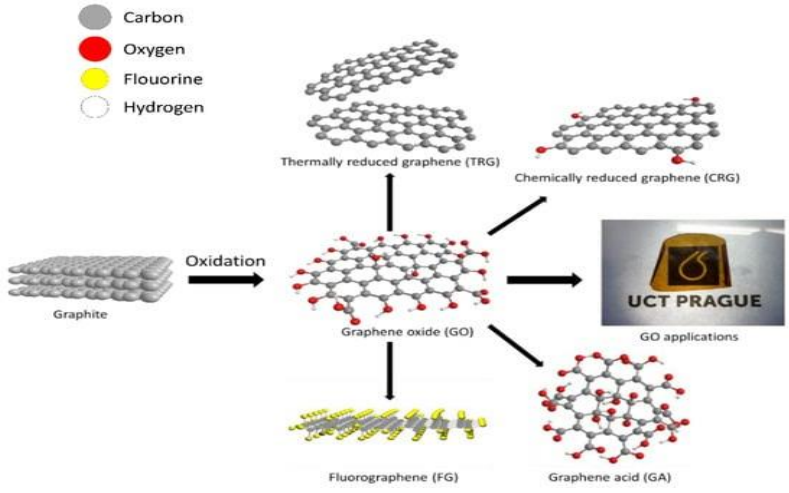

Figure 1. Scheme of preparation and utilization of GO (colors of atoms: grey—carbon, red—oxygen, yellow—fluorine, white—hydrogen). Reprinted with permission from [49].

3. Applications

3.1. Application of graphene and GO as electrical sensors.

It's because of the degeneration of both its CB (conduction-band), and VB (valance-band) graphene is classified as a zero bandgap semiconductor[46,50,51]. The conductance of graphene changes with the change in the following properties- i. Surface adsorption, ii. Enormous specific area of surface and iii. Low Johnson noise [2,52,53]. Recent findings indicate that Graphene can act as a very good sensor as it can detect various gases [54–57] and biomolecules [58–61]. As graphene can adsorb other molecules on the surface, charge transfer can occur where Graphene is capable of playing the role of either a donor or an acceptor, which can result in a shift in the material's Fermi levels, carrier density, and, ultimately its electrical resistance. Thus it can be shown a simple graphene-based FET which can sense ammonia gas and source-drain current (I_{ds}) can be changed concerning gate voltage (V_{gs}) at a different time in the presence of ammonia [62]. Initially, the Dirac point (V_D) appeared on the 0V. After 5 minutes, it appears at -20V and finally shifts to -30V. The above result gives evidence about the adsorption of ammonia on the surface and the formation of n-doped graphene. FET device and the concentration of the molecule adsorbed was 8×10^{13} cm^{-2} after 30 minutes. Experimentally it can be proved that NH_3 and CO behave as donors, whereas NO_2 and H_2O behave as an acceptor [55,63].

3.2. Application of graphene and GO asan electrochemical sensor.

Graphene and its oxide GO can form an excellent redox couple as they can show a wide range of electrochemical potential. After modifications like electrodeposition, electrochemical doping, and polymerization, graphene materials become effective for the electrochemical sensor. The electron transfer phenomenon is important yet challenging for preparing electrochemical biosensors as it is not an easy process [63]. The enzyme's activity may be diminished during the movement of electrons from the electrode to the enzyme's redox center, which is linked to a protein [64,65]. Several nanomaterials may be used to immobilize enzymes to carry forward the process of electron transfer without losing the biotic activity of the enzyme [66–69]. Graphene has been chosen as one of the most efficient nanomaterials owing to its distinctive 'honeycomb' lattice structure and large enough surface area on the basal plane [70]. The enzymatic reaction has been carried out with graphene as nanomaterial conjugated with metallic nanoparticles like gold (AuNPs), platinum (PtNPs), Iron-oxides (FeONPs), Nickel (NiNPs), copper (CuNPs), and palladium- (PdNPs) to develop nanocomposite on the surface of the electrode which can sense glucose, hemoglobin, and cholesterol [71–77].

The graphene-based electrochemical sensors are exceptional among others in terms of their fast electron transfer capacity, the LOD (limit of detection), and the ranges at which they are capable of operating. For these mentioned qualities, the graphene-based electrochemical sensors[78] can detect even a very small amount of ascorbic acid, uric acid, and dopamine type of biomolecules[79]. Nowadays, using chemically modified GO in GCE yields superior results in detecting free DNA's four base pairs[39]. By anchoring functionalized polydopamine (MIPDA)-coated platinum cobalt (Pt-Co) on the surface of GO, Cheng *et al.* created a new electrochemical sensor to detect tartrazine (TZ), which is genotoxic and cytotoxic to human health. The sensor responded linearly in the ranges of 0.003-0.180 and 0.180-3.950 M under optimal circumstances, and its limit of detection was 1.1 nM (S/N = 3). The excellent

repeatability and persistence of the sensors were also attributed to a synergistic interaction between the GO matrix and the polymeric imprinting unit[80]. Erdem and his coworkers designed GO- composite consisting of ionic liquid-based altered pencil-graphite electrodes as promising and highly convenient for detecting the BRCA1 gene. The lower detection limit (LOD) for the BRCA1 gene was computed in the range of concentrations of 2-10 g/mL and reported to be 1.48 g/mL. The sensor's sensitivity was determined to be 1.49 A mL/ g cm. Also, the GO-IL composite may have better electrocatalytic properties and a bigger surface area that is active electrochemically than either the untreated electrode or the modified GO-electrode alone[81]. Manikandan *et al*. revealed that electrochemically deposited Au-supported fluorine-doped rGO (Au-FrGO) modified glassy carbon electrodes to detect natural vanilla, a typical flavoring additive, and strong oxidant. The Au-FrGO nanocomposite had a considerably greater electroactive surface area and transported electrons much more quickly than Au NPs and FrGO-modified GCE. Despite tremendous improvements in the performance of graphene-based composite nanomaterials-modified electrodes as electrochemical sensors, there are still certain hurdles for future research as electrochemical sensors. The size, morphology, redox level, pureness, structural defects, and extent of dispersion all of these factors have a substantial bearing on how efficient GO-based electrochemical sensors are.

Some graphene-combined gold nanoparticle-based electrochemical biosensors are arranged in Table 1 [82].

Table 1. Graphene-combined gold nanoparticles-based electrochemical biosensors reproduced from Ref [82].

Biosensor structure	Metallic nanoparticle	Enzyme or protein	Analyte	Linear range (M)	LOD (M)	Sensitivity	Stability (days)	References
AuNPs/GR/ HRP/Chit/ GCE	AuNPs	HRP	H_2O_2	5×10^{-6}–5.13×10^{-3}	1.7×10^{-6}	–	21	[83]
PANI/HRP/ GR–CNT–Nafion/AuPt NPs/GCE	AuPtNPt	HRP	H_2O_2	5.0×10^{-7} – 1.0×10^{-4}	1.7×10^{-7}	3.7×10^{2}µA mM−1	30	[84]
Hb/AuNPs/ GR–Chit/ GCE	AuNPs	Hb	H_2O_2	2×10^{-6}–935×10^{-6}	0.35×10^{-6}	347.1 mA $cm^{-2}M^{-1}$	30	[85]
GR/AuNPs /GOD/Chit film-AuE	AuNPs	GOD	Glucose	2×10^{-4}–4.2×10^{-3}	180×10^{-6}	99.5µA cm^{-2} mM^{-1}	15	[86]
GR/AuNPsTyr-Chit/ GCE	AuNPs	Tyr	Bisphenol A	2.5×10^{-9}-3.0×10^{-6}	1×10^{-9}	3.597 mA mM^{-1}	90	[87]
AChE/AuNPs – PPy–RGO/ GCE	AuNPs	AChE	Paraoxonethyl	1.0×10^{-9} – 5×10^{-6}	0.5×10^{-9}	–	–	[88]
GOD-GR/ PANI/AuNPs GCE	AuNPs	GOD	Glucose	4.0×10^{-6}–1.12×10^{-3}	0.6×10^{-6}	-	20	[89]

Here are some graphene-combined TiO_2, Fe_3O_4, and NiO nanoparticles-based electrochemical biosensors arranged below in Table 2 [82].

Table 2. Electrochemical enzymatic biosensors fabricated from a combination of graphene and graphene oxide with metal and metal oxide nanoparticles.Ref[82].

Biosensor structure	Metallic nanoparticle	Enzyme or protein	Analyte	Linear range (M)	LOD (M)	Sensitivity	Stability (days)	References
HbinChit[bmim]PF6TiO$_2$-GR/GCE	TiO$_2$-GR	Hb	H_2O_2	1×10^{-6}–1170×10^{-6}	0.3×10^{-6}	–	20	[90]
PANI-TNTs/[Demim]Br/Nafion/GOD/GCE	TiO$_2$ nanotube	GOD	Glucose	10×10^{-6}–2.50×10^{-3}	0.5×10^{-6}	177.16 µA mM^{-1} cm^{-2}	30	[91]
HRP-Au–Fe3O4/ GS–Nafion/ SPCE	Fe_3O_4–AuNPs	HRP	H_2O_2	2.0×10^{-5}–2.5×10^{-3}	1.2×10^{-5}	–	30	[92]
Fe_3O_4/RGO/Hb/ GCE	Fe_3O_4NPs	Hb	H_2O_2	4×10^{-6} – 1×10^{-3}	2×10^{-6}	0.0468 µA µM−1	–	[93]
Nafion/Mb/NiO/GR/CILE	Electrodeposited NiO	Mb	H_2O_2	2.13×10^{-6} – 248.2×10^{-6}	0.71×10^{-6}	–	21	[94]

3.3. Application of graphene as strain sensors.

The word strain means the deformation of an object or medium resulting from high pressure and stress. The function of the strain sensor is to convert the force, pressure, weight, and tension into measurable electrical resistance. Graphene is given more priority than any other conductive material as a component of strain sensors due to its unique structure that allows the creation of a pseudomagnetic field, and this field helps to shift the Dirac cones and reduce the Fermi levels. Thus graphene shows various applications as a strain sensor[95,96]. The formation of a pseudo-magnetic field helps detect changes in electronic structure. One of the very important reasons to use graphene composites as strain sensors is the high value of the gauge factor (G.F.).

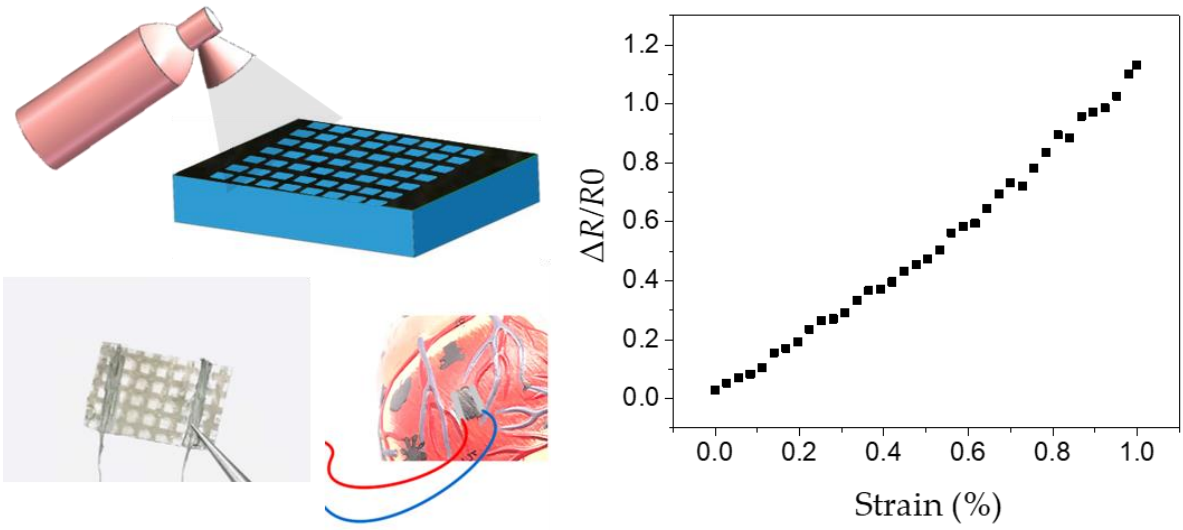

Figure 2. Graphene strain sensors could detect human movements. The lack of graphene growing and patterning processes hinders graphene strain sensors[101].

Graphene-based strain sensors are mainly available in fabricated form amalgamated with other materials, which are responsible for the amount of strain taken during the alteration of the unit resistance following the modification of the unit length[97,98], and strain amount is always more whenever it is used in a parallel direction to C-C whereas the strain is less on the perpendicular direction which is an attribute to the high bandgap. Nowadays, graphene films are produced on a variety of polymers for developing a piezo-resistive effect by applying strain which causes an irregular shift in electrical resistance. Mostly three types of polymer substrates are used to form different types of strain sensors[99–101]: PDMS (polydimethylsiloxane) with photolithography process; PET (Polyethylene terephthalate) with a drop-casting process; PI (Polyimide) with the thermal annealing process.

A researcher reported [100] wafer-scale, flexible, high-performance strain sensors that can be made in one step. rGO, when subjected to the "Light-Scribe DVD" burner, produced its converted graphene nano-sheets, which exhibit strain sensor's gauge factor (GF) is around 0.11. Graphene micro-ribbons (around 20 m wide and approximately 0.6 mm elongated) are employed as promising materials as strain sensors with a GF of 9.49. When the strain implications are modest, heavy GF is utilized, and low GF is used when the deformation is large. Graphene strain sensors scribed using a laser could have uses in the biomedical, artificial skin, and medicinal fields.

A researcher has shown [101] a soft-PET mask is used to splatter graphene solution to make the hypersensitive layer as gauge sensor. This foldable strain sensor is sensitive (at 1% strain gauge factor is 100), ultrafast due to low response time(400–700 s), durable (1000 cycles), and has low overflow (5%). These methods are suitable with curved substrates and should expand the use of flexible strain sensors.

Recently, rGO film-based strain sensors have received more attention for developing very sensitive strain sensors that are also flexible and stretchy. By manipulating the rGO film thickness and tailoring the physical separation between small rGO fragments, one can envision achieving remarkable sensitivity to mechanical stimuli on an rGO-based film surface composed of several over-connected networks of small rGO fragments where implemented strain causes separation throughout the junctions and resistance to change[102]. For example, rGO film and polyethylene terephthalate (rGO-PET) composite were created by drop casting PET on the surface of rGO film, where rGO is made by reducing GO using a 1.8W laser source. The gauge factor for the strain gauges that were made was found to be about 61.5, and the resistance values for stresses that were applied ranged from 0.01 to 0.04% and were fairly linear for each observation period.[102,103]Adding polystyrene nanoparticles to the rGO film changes the way the rGO particles are physically arranged and ends with a much more noticeable shift in resistance to distortion. As a consequence, at even 1.05% of strains, high GF values of 250 were found[104].

Graphene-derived strain sensors exhibit potent implications in many fields besides pressure sensors. It can be used as a healthcare device to detect any physiological change in our bodies. Recently weaving graphene fabric (GWF) with PDMS was used as a strain sensor to sense the activity of the throat muscles. GFW-based strain sensors are sometimes reported to have a G.F of 10^5, and graphene-based nano papers can also be used for strain sensors. Recent findings also indicate the change in electrical conductivity and relative strain up to 2200 $Scm^{-1}$and 540%, respectively, can be obtained using graphene-based strain sensors[105–115].Wearable sensors have indeed been connected to gloves, body parts, and skin for smart healthcare to analyze physiological functions of the body, such as monitoring heart rate, cardiac

cycle, intraocular pressure, and various other health-related situations. Because the mechanical qualities of piezoresistive materials, like elasticity and durability, are essential to wearable sensors, just a few materials are suitable for use in these devices. This discovery led to creating a wearable strain detector in the form of a graphene-woven fabric (GWF) on PDMS and medical tape composite. At strains of 0.2%, 2-6%, and >7%, 35, 103, and 106 are the gauge factor values measured by the sensor, respectively[116,117]. There has been a significant recent development in the design and analysis of graphene-based strain sensors, but it is clear that more work is needed in this area. Research in the future should concentrate on using synthesis to find solutions to existing challenges, improving the transfer and integration processes, and looking into how to make devices more sensitive and durable.

3.4. Application of GO as various gas sensors.

Many special properties are shown by GO exclusively due to its unique nonstoichiometric compositions with a ratio of 4:1 to 2:1 considering carbon and oxygen content and has a chemical formula ranging from $C_8O_2H_3$ to $C_8O_4H_5$ in the presence of epoxides hydroxyls and oxygen-related function groups on its large basal plane[118–121]. In the presence of these groups, GO can act as a good gas sensor as it can easily interact with various toxic gasses[122].

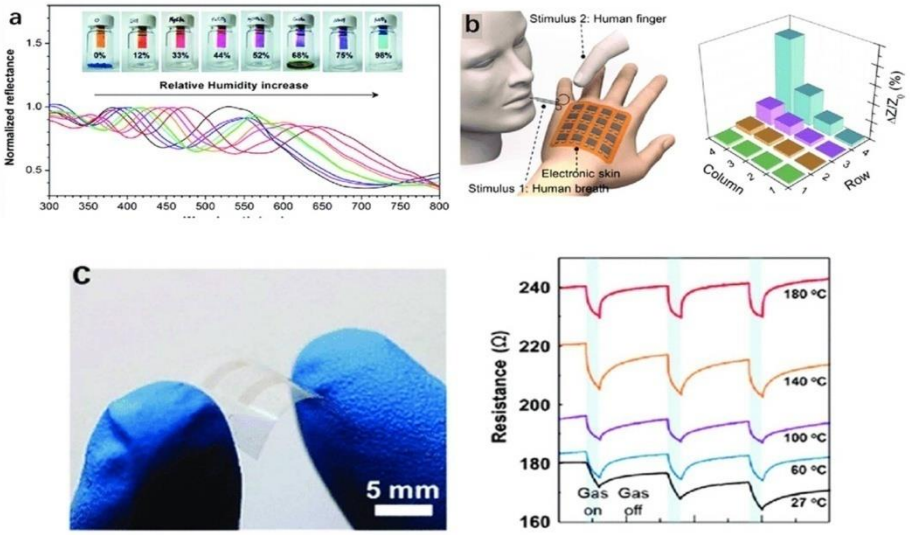

Figure 3. Graphene gas sensor (**a**) GO film that changes color when exposed to different RH. Reprinted with permission from[123] (**b**) A prototype showing how non-contact sensing works. Schematic plot of the relative change in impedance (Z/Z0) of each pixel in the gas sensor matrix. Reprinted with permission from [124] (**c**) A gas sensor made of graphene and PI. The graphene gas sensor's response curves to three 5 ppm NO_2 pulses at different temperatures. Reprinted With permission from [125].

In Figure 3, graphene-based sensors wearable-sensors which have tremendous potential, have been displayed.

In recent years, there has been a discernible trend toward incorporating graphene devices into wearable systems. These graphene devices have exceptional performance in terms of flexibility, biocompatibility, and electrical characteristics. Wearable graphene sensors have the potential to improve both the quality and quantity of the physiological signals they collect, making them an exciting development for the future of health care and telemedicine.[126]

The vicinity conductivity of the graphene and the potential for an inherent augmented sensing mode are two important benefits of the graphene-based sensor module [127]. When

hybridized with metal oxides, graphene's large specific surface area may also have synergistic benefits in attaining tailored gas sensitivity at room temperature, particularly on selection and sensitivity properties. In contrast, the exciton doping regions of graphene and rGO display nearly symmetric and ambipolar behavior (electrons and holes travel in opposite directions). Due to the molecules of oxygen and water that were immobilized, they additionally exhibited conducting characteristics *p* (hole) type.A *p-n* junction may also develop as a consequence of the arrangement of graphene sheets with an *n*-type metal oxide. The result would be a unique nanostructure with high electrocatalytic capabilities, a huge surface area, and an excellent absorption capacity [128]. The semiconductors 'surface continues to absorb electrons from n-type metal-oxides when they are put in an environment with oxidizing gases. The electrical resistance rises due to the wider Electron Depletion Layer (EDL). The thickness of the EDL is decreased, as is the resistance of the sensing material when they are put in an environment with reducing gases, which act as a donor of electrons at the metal-oxide interface.

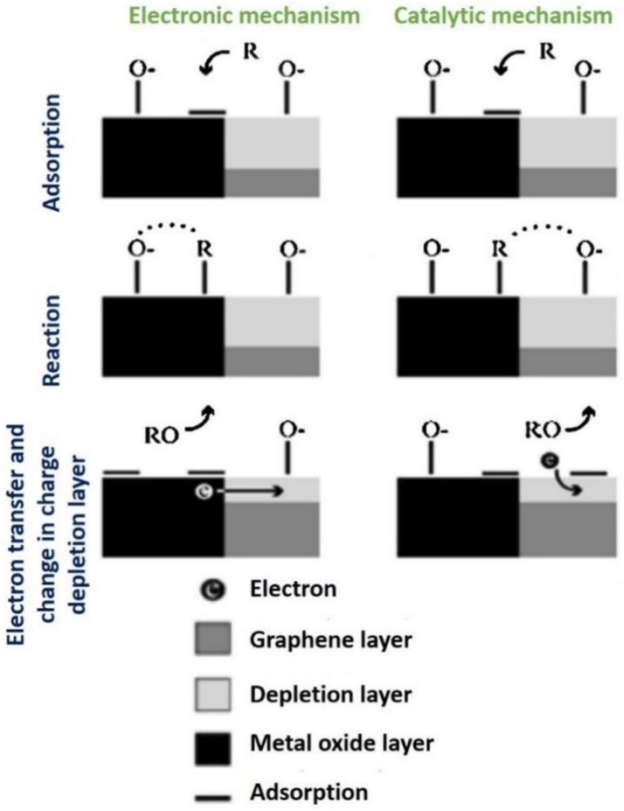

Figure 4. The basic processes of the electrical and catalytic interplay between the graphene-based gas-sensing layers and the metal oxide are depicted in this schematic diagram. [reprints with permission [128].

On the other hand, in the oxidizing gas environment, the resistance of p-type metal-oxides decreases because of an increase in the breadth of the Hole Accumulation Layer (HAL) caused by the trapping of electrons through the metal oxide surfaces. Electrons are liberated into the metal oxides when introduced to reducing gases, narrowing the HAL and raising gas sensor resistance. The operating temperature impacts the metal oxide's kinetics, resistivity, and electron mobility, which substantially impacts how well metal-oxide-based gas sensors can detect gases. To comprehend this sensing process for graphene-related gas sensors, Chatterjee *et al*. suggested two hypotheses focusing on (a) oxygen ion sorption and (b) the presence of unoccupied oxygen [127].

$$O_2(Gas) + e^- \rightleftharpoons O_2^-(adsorption) \text{.....(1)}$$

$$O_2^-(adsorption) + e^- \rightleftharpoons O_2^{2-}(adsorption) \rightleftharpoons 2O^-(adsorption) \ldots\ldots\ldots\ldots (2)$$
$$CO + O^-(adsorption) \longrightarrow CO_2 + e^- \ldots\ldots\ldots\ldots\ldots\ldots\ldots\ldots\ldots\ldots (3)$$
$$2CO + O_2^-(adsorption) \longrightarrow 2CO_2 + e^- \ldots\ldots\ldots\ldots\ldots\ldots\ldots\ldots\ldots\ldots (4)$$

They have proposed the typical actions of graphene-based detectors in response to exposure to air and a reducing gas (R) (shown in Figure 4). Equation (4), which explains oxygen adsorption, is derived by utilizing Equations (1) and (2). When exposed to a reducing gas like CO, the reactions at surfaces that occur adhere to Equations (3) and (4).

3.4.1.GO as ammonia gas sensor.

In this era of high air pollution, harmful gases like ammonia and carbon monoxide can be detected by using GO as a sensor. This thought opens up new opportunities for young chemists to use GO exclusively as a gas sensor. According to the information provided by the Occupational Safety and Health Administration (OSHA), even in people with the most delicate respiratory systems, only 50-100 ppm of ammonia can cause irritation to the eyes, nose, and throat[129–132]. However, many commercial metal oxides are available to sense ammonia but fail to detect it properly due to high-temperature operation. They generally function at a range of 200-400°C; at this temperature, ammonia shows a short life, and thus specific selectivity becomes poor[133–136]. Besides this method, many other methods are available, like conducting polymers[137,138], carbon tubes[139], etc. But they also have the same problems of poor selectivity and lower response[140,141]. Complex processing and high fabrication cost are two major limitations of using carbon nanotubes as sensors[142,143].

Peng and Li found that graphene and its oxide can adsorb ammonia, but GO's adsorption energy is higher than graphene due to its hydroxyl and epoxide groups. When one hydroxyl group binds to the nitrogen of ammonia, it shows adsorption energy of ~ 0.529eV, whereas, with two hydroxyl groups, it shows higher values of ~ 0.603 or 0.840 eV[49]. A functionalized GO is prepared by a simple esterification reaction between MTA and GO in the presence of Dicyclohexylcarboiimde (DCC) and hydroxybenzotriazole (HOBt) as a catalyst. A one-hour ultrasonicated solution of DMF and 20 mg of GO is mixed with a homogenous solution of MTA and DMF solution, which was ultrasonicated, maintaining room temperature. This mixture was subjected stirred approximately ½ hour at 27°C, and after that, the solution was warmed to 70 °C and further continuously mixed for another 3 hours, followed by the addition of DCC and HOBt powder, and the as-produced mixture was then swirled for a further 36 hours to produce functionalized GO (FGO). This FGO powder is finally dried at 82°C, and by repeating the same process, TG50 and TG75 can be formed with different concentrations of MTA. In order to make the depositing material for sensor device fabrication, 30 mg as-synthesized functionalized GO dissolved in approximately 20 ml of DMF, and the mixture is ultrasonically stirred for 1 hour to homogenize. This suspension is used to coat the substrate of the sensor. The substrate was coated on both sides with aluminum electrodes for the electrical-measurement top. Now it is ready to detect ammonia gas. The detection of ammonia gas can be understood when there is a decrease in electrical resistance.

The prepared functional graphene oxide(FGO) can sense ammonia by the surface reaction between Ammonia and FGO surface, leading to strong chemisorption and physisorption. The transfer of charge involving the ammonia and the FGOsurface results in the creation of hydrogen bonds. This phenomenon is responsible for strong adsorption between Ammonia and FGO surface[144].

The ammonia and FGO surface adsorption may take place with four different kinds of phenomena where ammonia molecules can be adsorbed at different sites. Those sites are as follows -

The simple physical adsorption takes place at the hollow site of fluorine-doped GO(FGO). Due to the presence of an epoxide ring, ammonia can be adsorbed through chemical adsorption by the formation of NH_2 and H, which are formed by the dissociation of ammonia, and these fragments can be absorbed into the epoxide ring after breaking the epoxide ring. Finally, OH and NH_2 groups formed at the carbon and oxygen sites.

On the surface of FGO, there are various carbon defect sites where dissociated ammonia can be adsorbed as NH_2 and H fragments leading to the creation of C- H and C- NH_2 bonds through chemical adsorption.

There is another possible way where a hydrogen bond is formed between the oxygen of the ester group of FGO and the hydrogen of ammonia.

The whole sensing mechanism, with the help of Langmuir-Blodget (LB) methods on the SiO_2/Si wafer surface, shows no change in sensing with changing the concentration of MTA[145].

3.4.2. GO as hydrogen gas sensor.

Metal oxide-based nanostructures are considered the best material for sensing various gases because of their better surface area and fast sensing capacity, which opens up a new possibility to incorporate this idea into electronic nose devices[136,146–149]. The commercially available metal oxide-based micro structures require a very high temperature and a large enough space to accommodate the whole system. These two major problems need to be modified so the system becomes portable and can operate at room temperature[146,148,150,151]. The sensing based on fabricated metal oxide nano and microstructures is also limited by lower sensitivity at room temperature[152–156]. Thus temperature is one of the important key factors for sensing operation[157]. However, Zhang and his team made novel membrane graphene-based composites with zeolitic imidazolate framework-8 membrane stayed by vertically oriented ZnO nanorods with extremely high H_2 or CO_2 sensitivity[158]. The use of GO is quite popular for its unique,non-uniformly distributed structure, which makes the material full of pores, thus making it perfect for fabricating selective materials[153,159]. Rasch and his research team first proposed designing ZnO microwires (MW) using a wet chemical method with a nanoporous thin GO membrane of less than 20nm. These particular GO/ZnO MW devices work based on the mechanism of effusion of the gas molecules through the nanopores. The gas sensing mechanism was studied for different types of gases with different concentrations, like hydrogen and some volatile compounds, including methane, acetone, ethanol, etc. Hydrogen gas molecules gave the best response with a very high gas sensing capacity of 4 ppm[160].

T. Pustelny *et al*. investigated another H_2 sensing device of GO with a resistive structure. Due to lower chemical reactivity and good electrical conduction power, gold is chosen to make interdigital electrodes of the resistive sensor structure. In between the gold layer and the resistive substrate of BK7, there must be a chromium layer of 35nm where the substrate is covered with chromium and gold, deposited through the Electron-beam physical vapor deposition (EBPVD) process. The width of the electrodes is around 90 µm, and they are separated by 110 µm. Modified Hummers GO was prepared, and the suspension of GO was applied on the prepared substrate using a spray coater from 20 cm apart so that the layer is hard

to notice at a glance. At a particular portion of the resistive structure, the Pd layer was deposited by the thermal evaporation method for further improvement of the sensor. For example, when the sensor is exposed to synthetic air with very low concentrations of H2 gas, the resistance (electrical) decreases irrespective of the gas concentration and the experimental temperature. In general, the temperature range is chosen from 21°C to 120°C. At lower temperature ranges, it only can sense H_2 when the concentration is more than 4%. Still, after increasing the temperature, the concentration and the batching gas may be easily identified from the graph, as shown in Figure 5[161].

Zinc oxide (ZnO) is one of the most common metal oxides in the gas sensing area because of its unique properties, such as n-type conductivity, low toxicity, ease of synthesis, high availability, good thermal stability, and high mobility of electrons [56,57]. Duan *et al.* demonstrated that RGO-supported Pd-SnO_2 (rGO/Pd-SnO_2)porous ternary nanocomposites have outstanding sensitivity and selectivity toward hydrogen response of 32.38 toward 200 ppm hydrogen at 360°C. The as-synthesized rGO/5.0 Pd-SnO_2 composites produced the best hydrogen sensing property owing to synergistic effects. Particularly, the 5.0 Pd-SnO_2/rGO sensitivity to 0.5 ppm (500 ppb) hydrogen reached 2.4, demonstrating the high potential in sensing incredibly low hydrogen concentrations. [162]

Table 3. Graphene (e.g., GO, rGO) and metal oxide semiconductor (MOS) based hydrogen gas sensors: a comparison of sensing performances. The sensor response is defined by the equation provided unless otherwise noted (1). (*) Obtaining the sensor's response in the form R a /R g. (**) Since no explicit recovery durations were provided in their articles, authors had to extrapolate these values using published sensor response curves. CVD stands for chemical vapor deposition, and RT stands for room temperature. Reprinted with permission from [163].

Ref. Nr.	Sensor Material	Operating Temperature	Method	Low Detection Limit	Response/Recovery Time (Response) at H_2 %	Literature
1	ZnO/G	150 °C	Hummer's method	200 ppm	22/90 s (3.5 *) at 200 ppm	[164]
2	ZnO/GO	RT	simple wet-chemical coating technique	4 ppm	114/30 s (3.42 *) at 1000 ppm	[160]
3	ZnO/rGO	RT	Electrochemical exfoliation	100 ppm	21.04/47.09 s (484.1% *) at 100 ppm	[165]
4	ZnO/rGO	250 °C	Modified Hummers method [C23]	100 ppm	−/− (30%) at 500 ppm	[166]
5	ZnO/Ag/Pd/rGO	150 °C	Modified Hummers method	100 ppm	10/14 s (59%) at 100 ppm	[167]
6	ZnO/rGO	150 °C	Modified Hummers method	100 ppm	33/19 s (46%) at 100 ppm	[167]
7	Ag/ZnO/rGO	150 °C	Modified Hummers method	100 ppm	45/27 s (51%) at 100 ppm	[167]
8	ZrO2/ZnO/rGO	150 °C	Modified Hummers method	100 ppm	15/16 s (52%) at 100 ppm	[167]
9	Pt/ZnO/rGO	100 °C	Modified Hummers method	50 ppm	12/412 s (99%) at 400 ppm	[168]
10	SnO_2/rGO	80 °C	Modified Hummers method	1000 ppm	15/61 s(1.58%) at 1000 ppm	[169]
11	Pd/SnO_2/G	RT	CVD	2%	50/100 s (11%) at 2%	[170]
12	SnO_2/G	RT	CVD	2%	18/12 s (0.35%) at 2%	[170]

Ref. Nr.	Sensor Material	Operating Temperature	Method	Low Detection Limit	Response/Recovery Time (Response) at H_2 %	Literature
13	Ni/ZnO/rGO	150 °C	Hummer‘s method	1 ppm	28/320 s (63.8%) at 100 ppm	[171]
14	CuO/rGO	RT	Thermal heating from GO at 180 °C	50 ppm	80/60 s (12%) at 1500 ppm	[172]
15	TiO_2/G	125 °C	Hummers’ chemical method	5000 ppm	16/61 s (18%) at 5000 ppm	[173]
16	MoS_2/rGO	60 °C	Modified Hummers method	200 ppm	261/260 s (15.6%) at 200 ppm	[174]
17	Pd/SnO_2/rGO	RT	Modified Hummers method	100 ppm	600 s/>2000 s ** (55%) at 10,000 ppm	[175]
18	SnO_2/rGO	60 °C	Modified Hummers method	200 ppm	119.6 s/265 s (19.6%) at 1000 ppm	[176]
19	Pd/WO_3/rGO	100 °C	Modified Hummers method	100 ppm	52/35 s (150 *) at 500 ppm	[177]
20	Pd/WO_3/G	RT	CVD-Method	0.1%	13/43 s(90%) at 4%	[177]

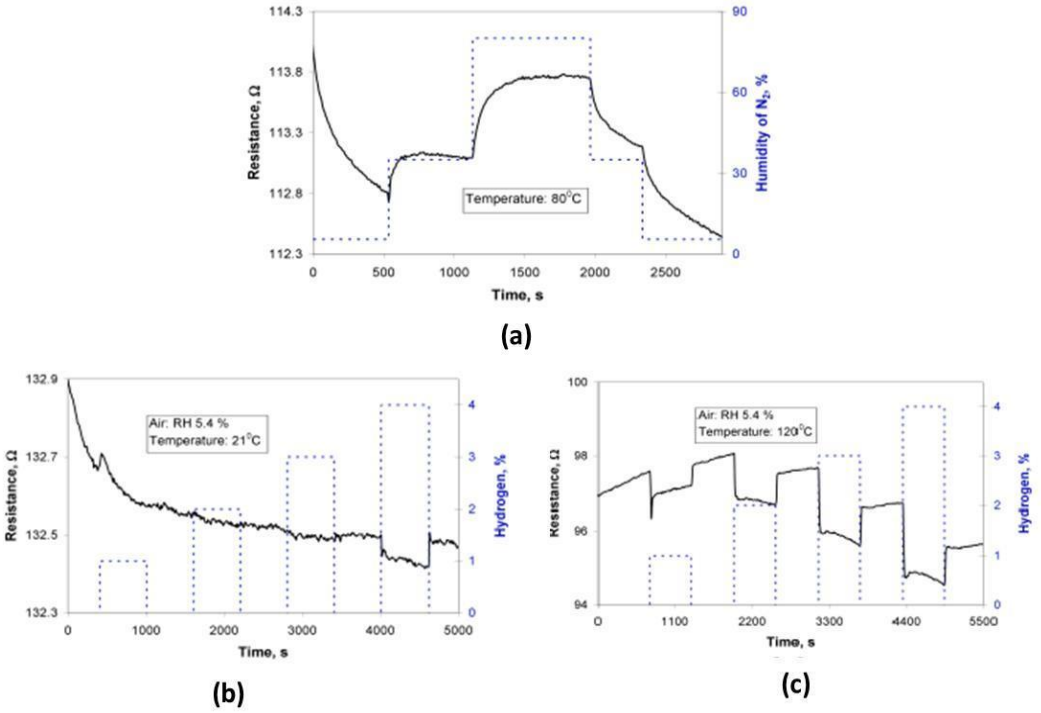

Figure 5. a) At 80°C when only humid N_2 is passed through the sensor, then the change in resistance with time, **b)** at 21°C, when 25% H_2 gas is passed through the sensor, maintaining the humidity at 5.4% then the change in resistance with time, c) at 120^{0}C when 25% H_2 gas is passed through the sensor maintaining the humidity at 5.4% then the change in resistance with time. Image adapted with permission from [161].

3.4.3. GO as nitrogen dioxide gas sensor.

NO_2 gas is toxic, and the production of this gas is high due to the increase in the use of fossil fuels in this era of urbanization and industrialization[178,179]. NO_2 is an air pollutant[180,181]. Some recent findings show that SnO_2, CuO and ZnO can be used as a sensor layer[182–184].On the other hand, the same kind of resistive sensor structure using GO, investigated by T. Pustelny *et al.*, was used for H_2 sensing and NO_2 sensing. NO_2 is a very toxic environmental gas that can be detected using this sensor. The resistance (electrical) of the

device reduces in the presence of NO_2 gas. Still, it requires more time to detect in comparison to H_2 because the sensor only senses NO_2 when the sensor structure is affected by NO_2. The detection of NO_2 also depends on temperature. When the temperature is set to 50°C, then resistance changes in wider ranges, but when it is set to 120°C, the gas atmosphere changes at a shorter time range; thus, resistance change is not as wider as in the previous case, as shown in Figure 6[161].

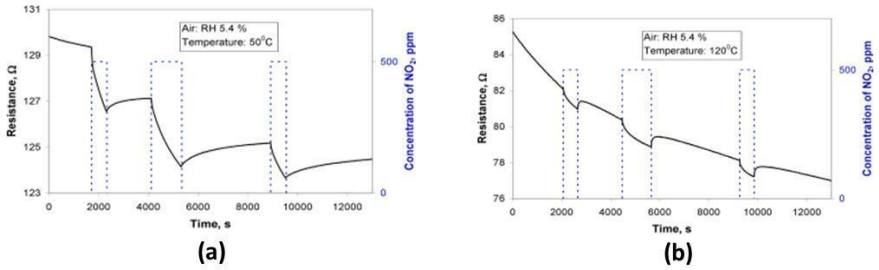

Figure 6. (a) at 21°C when 25% NO_2 gas is passed through the sensor maintaining the humidity at 5.4%, then the change in resistance with time;**(b)** at 120°C when 25% NO_2gas is passed through the sensor maintaining the humidity at 5.4% then the change in resistance with time. Image adapted with permission from [161].

Using paper substrates, low-cost gas sensors based on rGO were reported by Hassinen *et al.* to detect NO_2 at a smaller scale (ppm levels).The sensing behavior of rGO is affected by the thickness and shape of the r-GrO flakes[185,186]. One major disadvantage of using rGO in gas-sensing systems is its piteous specificity. However, it has been demonstrated that functionalizing rGO with metal or metal oxide nanoparticles improves its sensitivity[186,187]. Recently Jang Joo *et al.* asserted that the combed form of Au electrodes sputtered on the surface of silicon substrate were modified with narrow graphene oxide nanoribbons (GONR), and MoS_2nanospheres exhibit improved ability to detect NO_2 gas. The MoS_2 nanospheres were synthesized *via* the hydrothermal method and then deposited over the thin layer of GONR to decorate it. At room temperature, the unmodified and MOS_2 decorated GONR thin films can detect 10 ppm of NO_2 with 33% and 250% sensitivity, respectively[188]. Park *et al.*reported chitosan anchored rGO (rGO-CS) as a flexible and disposable paper-based gas sensor to detect toxic gas like NO_2. The chitosan molecules, which serve as a dispersion and reduction agent and support material, are responsible for the composite's ability to be easily bent and molded into various shapes as it is created. Due to its adhesive features, this composite can also be applied to paper, making it useful in various disposable activities. They reported that the above-mentioned composites could detect NO_2 in a concentration range of 0-100 ppm with a detecting limit of one ppm[189].

3.4.4. GO as mass gas (NO_2, SO_2, NH_3 and CO) sensor

GO can make another exciting mass-type gas sensor for different features of the 2D nanosheet as it contains various functional groups. Thus, it can easily detect NO_2, SO_2, CO, and NH_3[35,190–195]. Ultrasound dilutes and disperses GO nanosheets in simple deionized water (DI)at a controlled concentration. On quartz crystal microbalance (QCM) electrodes, dispersion is deposited. Then the substrate is added using a spray coating process maintaining a distance of 30cm at a fixed temperature of 170°C. Finally, it is hard-baked for the production of the mass-type gas sensor. All the gases, like NO_2, NH_3, SO_2, etc., are diluted in N_2, and finally, the frequency shift is measured. At first simple N_2 gas is flushed through the device at a rate of 200 sccm then any one of the test gas is flushed at the same rate, and now the frequency

shift is measured, and the process is repeated two more successive times. At first SO_2 gas was taken for the experiment, and it was checked with different concentrations of 2.5, 7.5, 10, 12.5, and 15 ppm, and the respective shift of frequency was found at 2.9, 4.3, 7.4, 10.1, and 15 Hz. It is also found that with an increasing concentration of SO_2, the frequency shift increases along with response time. As an example, when the concentration was kept at a range of 5-15ppm, the response time range was between 65 to 80s. The same kind of procedure was followed for other gases like NO_2, NH_3, and CO, which all showed excellent results with the same range of concentration, where they give the same frequency change[196]. Another study revealed that hydrothermal treatment of graphite and $HAuCl_4$ yields rGO/Au hybrid-nanocomposite that exhibits excellent NO_2 sensor at 50 °C, as shown in Figure 7 [197]. This above-mentioned nanocomposite is more sensitive, faster, and more reproducible than pure rGO.

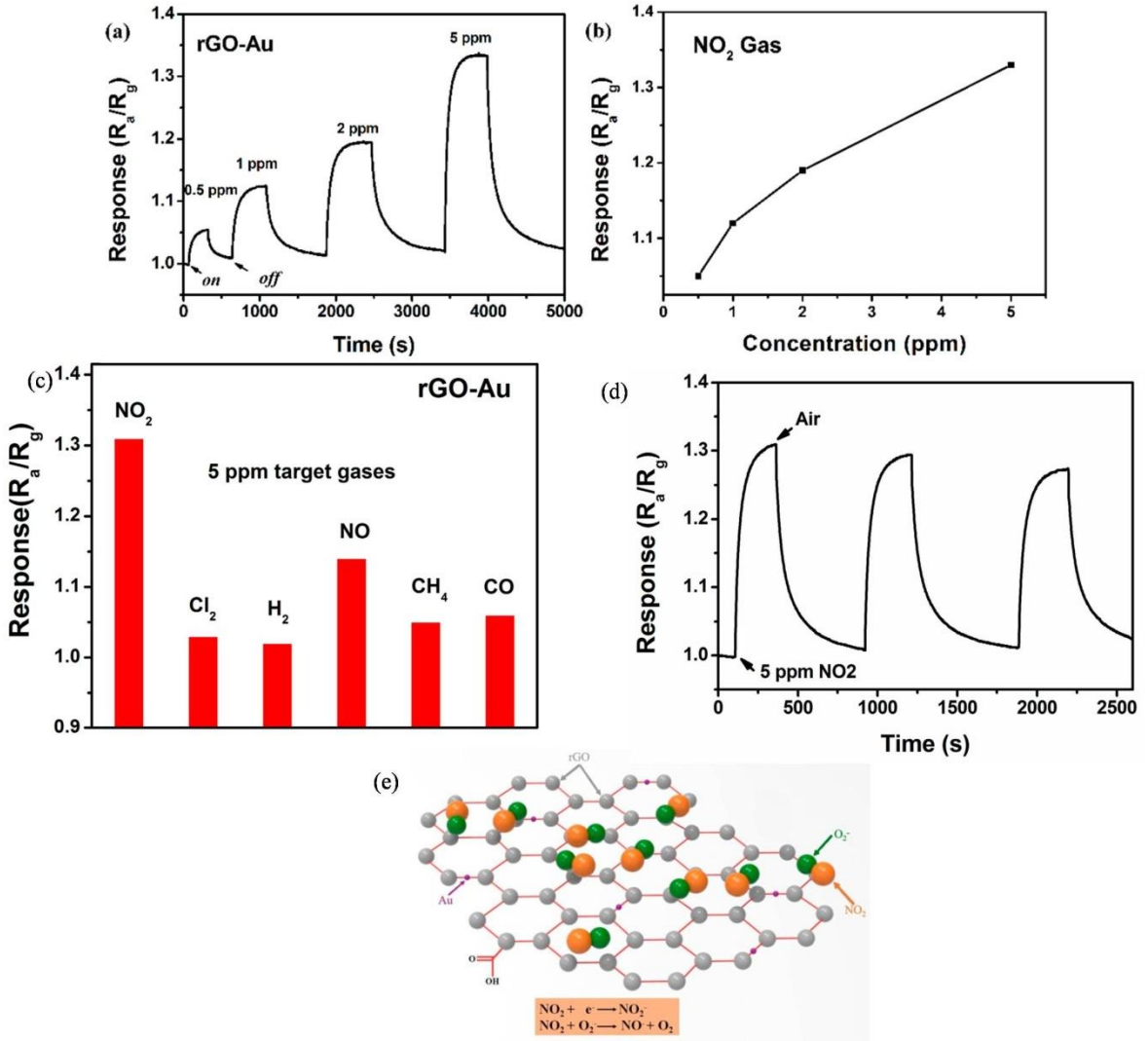

Figure 7. (a) Dynamic NO_2 sensing transients curve of the rGO/Au-based sensor to 0.5–5 ppm NO2 at 50 °C; (b) The responses of the rGO/Au-based sensor to 0.5–5 ppm NO2 at 50 °C, (c) The responses of rGO/Au based sensor to 5 ppm of different gases at 50 °C, (d) The reproducibility of the rGO/Au sensor on successive exposure (3 cycles) to 5 ppm NO_2 at 50 °C. and (e) The scheme of the proposed gas sensing mechanism: the adsorption behavior of NO_2 molecules on the rGO/Au nanocomposite. All the figures and captions are reprinted with permission form [197].

Hydrothermally deposited ZnO nanorods on the surface of GO-form composite (GO/ZnO–NR) were proven as a superior sensor to detect H2 and SO2 at room temperature with a linear response below 100 ppm. The SO2 sensor's delayed response and recovery

durations are caused by firmly adhering SO3 species. A detailed mechanistic approach is shown in Figure 8 [198].

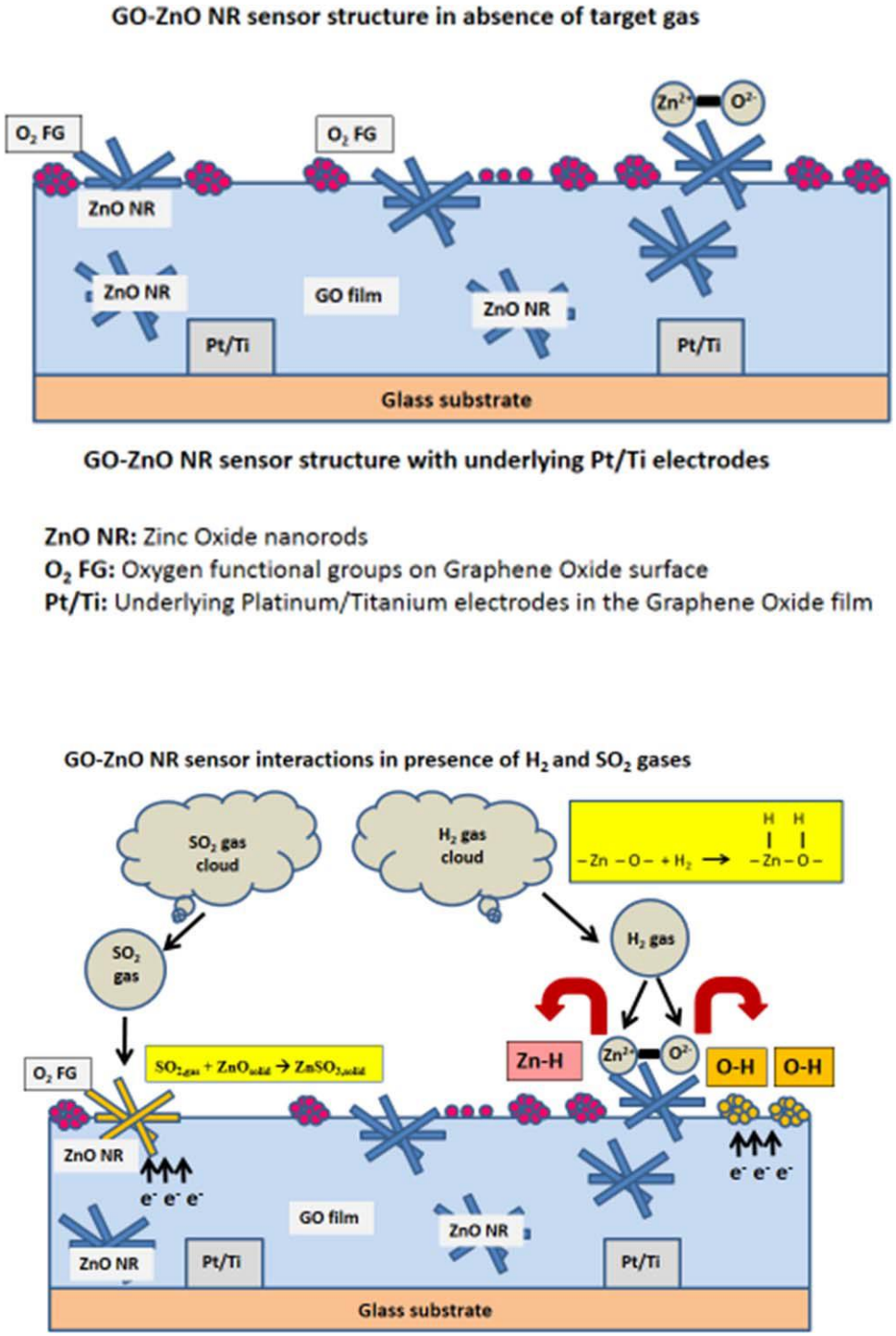

Figure 8. Graphical representation of the gas sensing mechanism of GO-ZnO-NR composite sensor (a) in the absence of H_2 and SO_2 gases (b) in the presence of H_2 and SO_2 gases. Reprinted with permission from [198].

Figure 9 shows that nano composites based on Pt-anchored reduced GO exhibit an excellent radio frequency identification (RFID)-based wireless smart-sensor for sensing hydrogen gas at concentrations as low as 1 ppm.

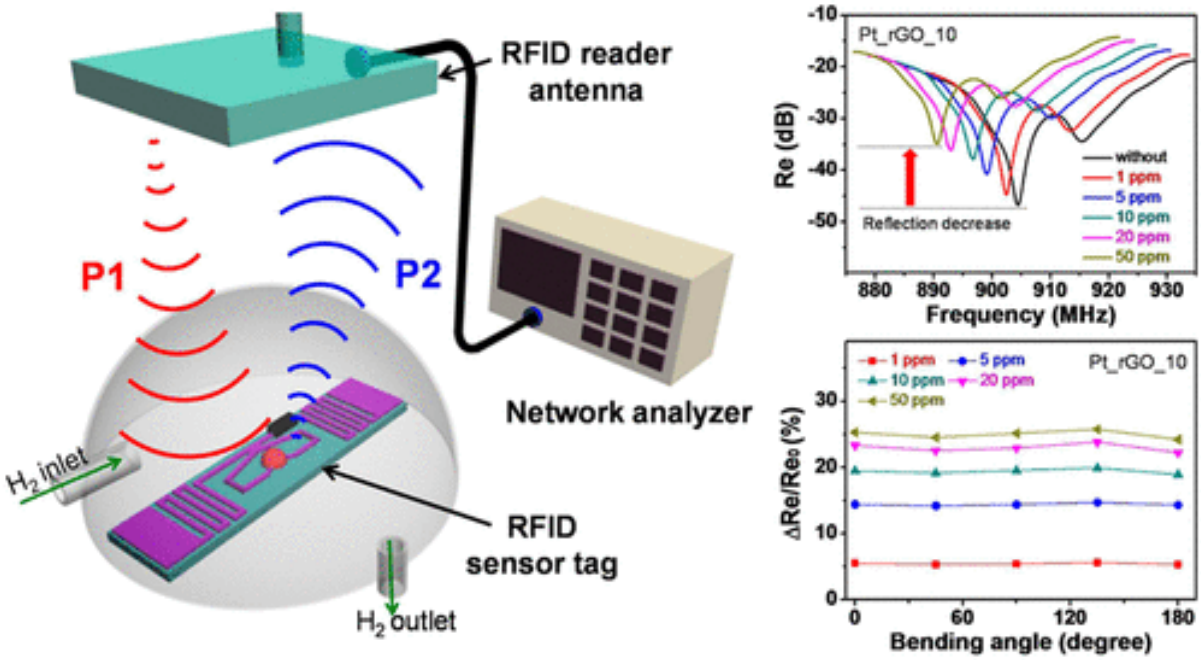

Figure 9. A presentation of an RFID-based wireless system to sense hydrogen gas by using Pt/rGO as a sensing material Reprinted with permission from [199].

Researchers[194] reported the manufacture of H_2sensors for practical purposes based on one-dimensional multi-walled carbon nanotubes (MWCNTs) adorned with noble nanomaterials and 2D graphene produced through a straightforward drop casting method. For example, Pt-anchored functionalized-graphene nano-sheets (Pt/f-G) and Pt-anchored functionalized MWCNTs(Pt/f-MWNT) were used to study as H_2 sensors. Analyses performed on (Pt/f-G) for the purpose of hydrogen sensing at a low sensitivity level of 4 vol% hydrogens in air demonstrate a reaction time that is comparable to that of (Pt/f-MWNT) but with a twofold improvement in sensitivity at room temperature.

Figure 10. Graphene-based ultrafast sensor systems for wearable electronic devices. Reproduced with permission from [201].

Over multiple hydrogenation and dehydrogenation cycles, these sensors were likewise found to retain their initial sensitivity.

Researchers[200]have made a stretchy, translucent gas sensor from a hybrid composite of Ag-Graphene (Ag-G) composited. Owing to its excellent tensile and opto-electronic properties, the sensor is durable even under significant mechanical distortion (up to 20% strain). Bluetooth or an inductive antenna enables wireless sensor functioning. The system may be placed onto nonplanar substrates, such as a wristwatch, a light bicycle, and living plant leaves, attributable to the materials' resilience, advancing toward the forthcoming generation of sensor technologies to be used in "the Internet of Things" [200].

A schematic representation of graphene and its composite materials was depicted in Figure 10 [201] as an ultrafast sensor to construct wearable electronic devices.

The most concerning feature of graphene/graphene oxide derivative-based sensing operations for hazardous sensing applications is that the higher working temperature cannot be reduced. Furthermore, moisture is vital in the sensor module, as the sorption of H_2O molecules would alter the target analyte's sorption and response on the sensor's surface, diminishing the sensor's responsiveness. The long-term focus could be on improving moisture responsiveness to prepare a harmful gas detector with superior performance, and humidity resistance appropriate for potential implementation, particularly in areas where the humidity level is very high. Future advancements in rGO-based sensitive information are anticipated to serve a crucial function as a gas-sensitive material, making it even more valuable for various studies.

Many types of Graphene derivatives are used as gas sensors, and hybrids and composites are currently of great interest. However, the feasibility of scaling up technical processes must be thoroughly examined based on effectiveness. It is crucial to incorporate fabrication techniques into the analysis of sensors. Though there are several approaches have been employed to sense various gas like NH_3, H_2, H_2S, SO_2, NO_2, etc., at room temperature by graphene and its derivative-based sensors, the sensitiveness, scale-up, response along with recovery time of the sensors are the major issue for its commercialization.

3.5. Graphene-derived membrane for surface stress sensors (G-MSS).

Graphene's huge surface area and chemical modification capabilities make it ideal for gas detection. In this section, we have articulated G-MSS as a sensing platform. GO's viability as a gas-detecting material for static mode nanomechanical sensors and its water vapor selectivity have been published [202], as displayed in Figure 11, which illustrates the implication of G-MSS as a sensing platform. After a comparative analysis of GO, rGO, and graphite powder sensing responses, they examined the MSS sensing process. GO can be used in static mode nanomechanical sensors for gas sensing; GO-coated MSS responded clearly to solvent vapors, especially water vapor. Oxygen-containing functional groups improve GO's ability to absorb oxygen, as shown by comparing GO, rGO, and graphite structures, resulting in its high selectivity and sensitivity to water with gas detection at 100 ppm. Using GO-coated MSS components may facilitate the creation of handheld instruments for determining water and hydrophilic gas concentrations. As a sensing material, GO has also been demonstrated to have promise in static nanomechanical sensors.

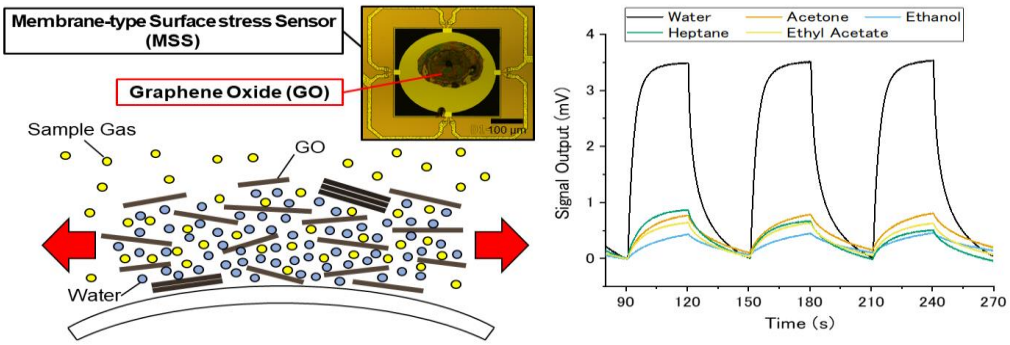

Figure 11. MSS as a sensing platform and GO as a gas sensing material. As a gas-detecting material, chemically modified graphene with low conductivity has been employed, and five distinct gases have been measured. Reproduced with permission from [202].

3.6. Bio sensors.

Biosensors are increasingly being used to detect biochemical molecules in the human body, food products, and other relevant fields. Using new nanomaterials' chemical and electrical features, biosensors are being made more sensitive and efficient[35]. In addition, biosensor applications benefit greatly from selectivity, exactness, and a minimum detection limit.

Graphene is superior to other materials for biosensing fields for its many advantageous properties. The existence of ripples and folds boosts the chemical adaptability of graphene materials. This means that more detection or analyte components can be added to the surface of graphene [203]. Graphene's sp^2-hybridized carbon atoms and monolayer structure make it a unique material that can be changed in many ways to improve its performance. This means that it can be made to fit the needs of each biosensor. Graphene's monolayer structure and the attraction sites created by its bonds make it a good candidate for these sorts of changes[204]. Attaching organic groups like chromophores to graphene's surface is one way to modify its electrical properties, while tampering with graphene's extended character is another[205].

Graphene and its derivative-based systems are also great for biosensing since they can immobilize a variety of bioreceptors, either covalently or non-covalently. Noncovalent interactions, like stacking, hydrogen bonding, and electrostatic repulsion, allow single-stranded DNA to bind on the surface of graphene from its ring-structured nucleobases. Amine protein groups serve as chemical "glue" that binds proteins to graphene oxide's carboxylic groups[206].

The electrical characteristics of graphene for their sp^2 hybridized structure include free-moving bonds. As a result of the rapidity with which electrons may be transferred between a bioreceptor and a transducer manufactured from graphene, electrochemical biosensors can achieve a very high level of sensitivity[202].

Strong C-C bonds contribute to its high mechanical strength, making it harder than diamonds. Furthermore, the material's softness and pliability are enhanced by Van der Waals forces. Graphene's unique ability to be both rigid and malleable has made it a popular choice for use in wearable-flexible biosensors [130].

Due to their enhanced signal output, graphene and its derivative are becoming increasingly significant in nano-sensor applications[202]. DNA, lipids, peptides, viruses, antibodies, and heavy metal ions are just some of the many chemical and biological entities that graphene can successfully detect (Figure 12) [202].

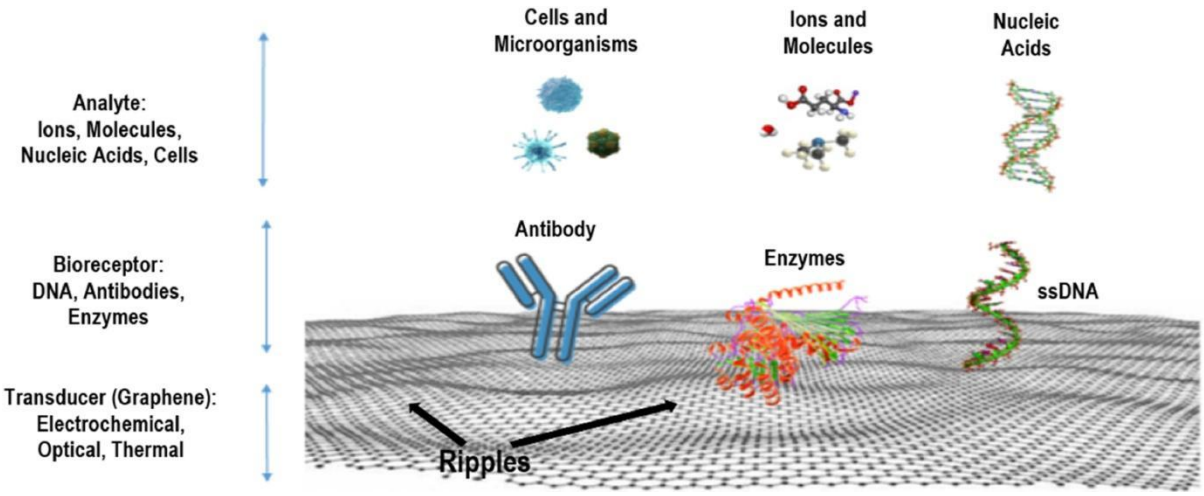

Figure 12. Biosensor transducers employ graphene. Graphene can immobilize DNA, antibodies, and enzymes. Graphene can detect ions, chemicals, nucleic acids, and cells [202].

A bio-receptor is the component that makes up a biosensor that recognizes the analyte, and a transducer turns the chemical signal into an electrical signal[207-208]. Aptamers, DNA, cells, and antibodies are bioreceptors. Biosensor transducers employ graphene. An analyte binds to a bioreceptor, generating a signal (temperature, light, or pH change). Bioreceptors on a transducer transform a chemical stimulus into an electrical signal (e.g., graphene).[200,209,210]Graphene transducers boost the electrical conductivity of biosensors, electron transfer kinetics, and better surface area.[211].

Electrochemical, Fluorescent, Optical, particularly Surface-Plasmon-Resonance (SPR), along with Surface-enhanced Raman-Scattering (SERS) biosensors, are the most common applications of graphene and graphene-based materials, e.g., GO, rGO. In Table 4 [212] several examples of biosensors based on graphene are reported.

Table 4. Biosensors based on graphene[212].

Sensor Type	Target	Detection Method	Reference
Electrochemical	Glucose	Graphene/Nafion/Pt NPs/Chitosan/GOD	[213]
Electrochemical	Glucose	Graphene/GOD/chitosan	[72]
Electrochemical	Prostate Specific Antigen	Graphene sheet/Methylene blue/ Chitosan/Antibody	[214]
Electrochemical	Prostate Specific Antigen	Graphene sheet/Quantum dot functionalized graphene/antibody	[215]
Electrochemical	Pb(II)	Graphene field effect transistor/DNAzyme/Pyrene	[216]
Surface Plasmon Resonance	3-nitro-L-tyrosine	Graphene/Nickel	[217]
Surface Plasmon Resonance	Folic acid	Graphene	[218]
Surface Plasmon Resonance	ssDNA	Graphene/Gold nano urchin/ssDNA	[219]
Surface-enhanced Raman spectroscopy	Aristolochic acids	Graphene/Ag NPs/Fe3O4	[220]
Surface-enhanced Raman spectroscopy	Rhodamine B	N-doped graphene	[220]
Surface-enhanced Raman spectroscopy	Rhodamine 6 G/crystal violet/thiram	Graphene/Ag NPs/CuF	[221]
Optical	DNA	Graphene-MoS2/BK7 prism/Ag/SiO2/Au	[222]
Optical	Nitrate	Graphene/Optical fiber tip	[223]

The principle of bio-sensors is based on the interaction between the target analyte with senor material to produce noticeable signals. It was reported that the biomolecules such as glucose, DNA, RNA, and antibodies are quickly immobilized on the 2D flat surface of

graphene to facilitate interactions with the targeting molecules[60,224–226]. For instance, Dey *et al*. employed ferrocene-anchored GO sheet-based biosensors to detect cholesterol. The above-said sensors have better linear response and sensitivity[76]. Bagherzadeh *et al.* Constructed Pyrenebutyric acid NHS ester bonded armchair graphene nanoribbon (PBANHSE-AcGNR) derivative-based biosensors to ameliorate DNA hybridization sensing. Pyrenebutyric acid NHS ester (PBANHSE) impediment to the surface of graphene via the stacking of the pyrene group of PBANHSE through noncovalent interaction. The single-strand DNA (ss-DNA) was a trap on the surface of PBANHSE-GO via covalent interactions with PBANHSE. After the amine group in the probe DNA nucleophilically substituted 1-Hydroxysuccinimide, an amide bond was formed that allowed the probe DNA to be attached to PBANHSE. It was determined that functionalizing AcGNR with PBASE enhanced the sensor's conductivity. The above-mentioned sensor displayed 10% sensitivity at zero bias voltage and increased sensitivity when an appropriate gate voltage was used[227]. To detect large concentrations of artificial sweeteners like sucralose, Bathinapatla*et al*. created GO-modified glassy carbon electrodes assisted by laccase immobilized, p-amino thiophenol ZnO based biosensors (L/ZnO-thiophenol-GO/GCE). In Phosphate buffer (0.1 M) at pH 5, the aforementioned biosensors exhibit an eight-fold improvement in differential pulse voltammetry signals compared to the standard GCE. The strong binding of laccase to the surface of GO through high isoelectric point and nanodomain ZnO, which displayed enzymatic catalytic activity towards the oxidation of sucralose, was responsible for the signal enhancement[228].

Though GO and its functionalized derivatives have potential applications in the advancement of futuristic biosensing like glucose oxidase, cholesterol DNA, RNA, and so on, the substantial possibility to be explored in the long term is the increasing demand for the engineering of GO-based biosensors that allow monitoring and designed to detect analytes with high specificity and sensitivity to a great extent for little expense. GO-based biosensors should also be devised as point-of-care diagnostic devices or as an in-situ sensing platform for environmental assessment.

4. Conclusions

This mini-review articulates the synthesis and applications of graphene oxide, emphasizing its use as gas, electrochemical, and membrane-type surface stress sensors. Undoubtedly, graphene's future in the realms of gas detection and electrochemical sensors is Brobdingnagian. Graphene nanosensors have a promising future in industrial production as well as environmental remediation due to their benefits in sensitivity, selectivity, and compactness. Nonetheless, graphene's present large-scale exploitation still faces obstacles. There are two major challenges. First, there isn't any technology for preparing graphene sensing devices on a large scale. Second, graphene must be modified in various ways to make it more responsive to specific gases. Based on the current state of affairs, response time might be enhanced by: 1) boosting the high surface area by modifying the surface and integrating it with various nanomaterials; and 2) developing the optimal structure. As research continues, enhanced graphene-based gas-sensitive materials will hold an important place in the future of gas-sensitive materials and provide increasing advantages. Graphene-based systems arise as viable platforms for sensor implications, requiring continued collaboration within scientific groups such as chemistry, physics, and biology to facilitate their implementation.

Funding

Technical and financial support from the University of Engineering and Management Kolkata and financial support from Taif University's Researchers Supporting project fund (Project number TURSP-2020/266) from Taif University, Taif, Saudi Arabia, is gratefully acknowledged. SG is thankful to DST IC#3 Projects (DST/TM/EWO/MI/CCUS/15 & DST/TMD/HFC/2K18/06), while SG is also thankful to SERB Project (ECR/2018/000254) and SPARC Project (SPARC/2018-2019/P124/SL) for kind financial help. SB is thankful to MHRD and CSIR-UGC, respectively, for the JRF fellowships and is also thankful to the PMRF fellowship.

Conflicts of Interest

The authors declare no conflict of interest.

References

1. Martin, C.R.; Kohli, P., The Emerging Field of Nanotube Biotechnology.*Nat. Rev. Drug Discov.*, **2003**, *2*, 29–37, https://doi.org/10.1038/nrd988.
2. Geim, A.K.; Novoselov, K.S., The Rise of Graphene.*Nat. Mater.*, **2007**, *6*, 183–191, https://doi.org/10.1038/nmat1849.
3. Boehm, H.P.; Clauss, A.; Fischer, G.O.; Hofmann, U., Das Adsorptionsverhalten sehr dünner Kohlenstoff-Folien, *Z Anorg Allg Chem*, **1962**, *316*, 119–127, https://doi.org/10.1002/zaac.19623160303.
4. Boehm, H.P.; Setton, R.; Stumpp, E., Nomenclature and Terminology of Graphite Intercalation Compounds (IUPAC Recommendations 1994).*Pure Appl. Chem.*, **1994**, *66*, 1893–1901, https://doi.org/10.1351/pac199466091893.
5. Wintterlin, J.; Bocquet, M.-L., Graphene on Metal Surfaces, *Surf. Sci.*, **2009**, *603*, 1841–1852, https://doi.org/10.1016/j.susc.2008.08.037.
6. Van Bommel, A.J.; Crombeen, J.E.; Van Tooren, A., LEED and Auger Electron Observations of the SiC(0001) Surface.*Surf. Sci.*, **1975**, *48*, 463–472, https://doi.org/10.1016/0039-6028(75)90419-7.
7. Lu, X.; Yu, M.; Huang, H.; Ruoff, R.S., Tailoring Graphite with the Goal of Achieving Single Sheets.*Nanotechnology***1999**, *10*, 269–272, https://doi.org/10.1088/0957-4484/10/3/308.
8. Lu, X.; Huang, H.; Nemchuk, N.; Ruoff, R.S., Patterning of Highly Oriented Pyrolytic Graphite by Oxygen Plasma Etching.*Appl. Phys. Lett.***1999**, *75*, 193–195, https://doi.org/10.1063/1.124316.
9. Sim, Y.; Surendran, S.; Cha, H.; Choi, H.; Je, M.; Yoo, S.; Chan Seok, D.; Ho Jung, Y.; Jeon, C.; Jin Kim, D.; Han, M.-K.; Choi, H.; Sim, U.; Moon, J., Fluorine-Doped Graphene Oxide Prepared by Direct Plasma Treatment for Supercapacitor Application.*Chem. Eng. J.*, **2022**, *428*, 132086, https://doi.org/10.1016/j.cej.2021.132086.
10. Tabish, T.A.; Abbas, A.; Narayan, R.J., Graphene Nanocomposites for Transdermal Biosensing.*WIREs Nanomedicine Nanobiotechnology*, **2021**, *13*, https://doi.org/10.1002/wnan.1699.
11. Cao, J.; Chen, Y.; Zhang, J.; Wang, X.; Wang, J.; Shi, C.; Ning, Y.; Wang, X., Preparation and Application of Nanofluid Flooding Based on Polyoxyethylated Graphene Oxide Nanosheets for Enhanced Oil Recovery.*Chem. Eng. Sci.*, **2022**, *247*, 117023, https://doi.org/10.1016/j.ces.2021.117023.
12. Bolotin, K.I.; Sikes, K.J.; Jiang, Z.; Klima, M.; Fudenberg, G.; Hone, J.; Kim, P.; Stormer, H.L., Ultrahigh Electron Mobility in Suspended Graphene, *Solid State Commun.*, **2008**, *146*, 351–355, https://doi.org/10.1016/j.ssc.2008.02.024.
13. Morozov, S.V.; Novoselov, K.S.; Katsnelson, M.I.; Schedin, F.; Elias, D.C.; Jaszczak, J.A.; Geim, A.K., Giant Intrinsic Carrier Mobilities in Graphene and Its Bilayer, *Phys. Rev. Lett.*, **2008**, *100*, 016602, https://doi.org/10.1103/PhysRevLett.100.016602.
14. Lee, C.; Wei, X.; Kysar, J.W.; Hone, J., Measurement of the Elastic Properties and Intrinsic Strength of Monolayer Graphene. *Science***2008**, *321*, 385–388, https://doi.org/10.1126/science.1157996.
15. Wang, S.; Ang, P.K.; Wang, Z.; Tang, A.L.L.; Thong, J.T.L.; Loh, K.P., High Mobility, Printable, and Solution-Processed Graphene Electronics.*Nano Lett.*, **2010**, *10*, 92–98, https://doi.org/10.1021/nl9028736.
16. Balandin, A.A.; Ghosh, S.; Bao, W.; Calizo, I.; Teweldebrhan, D.; Miao, F.; Lau, C.N., Superior Thermal Conductivity of Single-Layer Graphene.*Nano Lett.*, **2008**, *8*, 902–907, https://doi.org/10.1021/nl0731872.
17. Li, X.; Zhu, Y.; Cai, W.; Borysiak, M.; Han, B.; Chen, D.; Piner, R.D.; Colombo, L.; Ruoff, R.S., Transfer of Large-Area Graphene Films for High-Performance Transparent Conductive Electrodes.*Nano Lett.***2009**, *9*, 4359–4363, https://doi.org/10.1021/nl902623y.

18. Becerril, H.A.; Mao, J.; Liu, Z.; Stoltenberg, R.M.; Bao, Z.; Chen, Y., Evaluation of Solution-Processed Reduced Graphene Oxide Films as Transparent Conductors. *ACS Nano*, **2008**, *2*, 463–470, https://doi.org/10.1021/nn700375n.
19. Hummers, W.S.; Offeman, R.E., Preparation of Graphitic Oxide.*J. Am. Chem. Soc.*, **1958**, *80*, 1339–1339, https://doi.org/10.1021/ja01539a017.
20. Ramamoorthy, H.; Buapan, K.; Chiawchan, T.; Thamkrongart, K.; Somphonsane, R., Exploration of the Temperature-Dependent Correlations Present in the Structural, Morphological and Electrical Properties of Thermally Reduced Free-Standing Graphene Oxide Papers.*J. Mater. Sci.***2021**, *56*, 15134–15150, https://doi.org/10.1007/s10853-021-06262-w.
21. Sieradzka, M.; Ślusarczyk, C.; Biniaś, W.; Fryczkowski, R., The Role of the Oxidation and Reduction Parameters on the Properties of the Reduced Graphene Oxide.*Coatings*, **2021**, *11*, 166, https://doi.org/10.3390/coatings11020166.
22. Esposito, F.; Sansone, L.; Srivastava, A.; Baldini, F.; Campopiano, S.; Chiavaioli, F.; Giordano, M.; Giannetti, A.; Iadicicco, A., Long Period Grating in Double Cladding Fiber Coated with Graphene Oxide as High-Performance Optical Platform for Biosensing.*Biosens. Bioelectron.*, **2021**, *172*, 112747, https://doi.org/10.1016/j.bios.2020.112747.
23. Jung, I.; Dikin, D.A.; Piner, R.D.; Ruoff, R.S., Tunable Electrical Conductivity of Individual Graphene Oxide Sheets Reduced at "Low" Temperatures.*Nano Lett.***2008**, *8*, 4283–4287, https://doi.org/10.1021/nl8019938.
24. Wu, L.; Shao, H.; Yang, C.; Feng, X.; Han, L.; Zhou, Y.; Du, W.; Sun, X.; Xu, Z.; Zhang, X.; Jiang, F.; Dong, C., SnS2 Nanosheets with RGO Modification as High-Performance Anode Materials for Na-Ion and K-Ion Batteries.*Nanomaterials*, **2021**, *11*, 1932, https://doi.org/10.3390/nano11081932.
25. Marcos-Viquez, A.L.; Miranda, Á.; Cruz-Irisson, M.; Pérez, L.A., Tin Carbide Monolayers as Potential Gas Sensors.*Mater. Lett.*, **2021**, *294*, 129751, https://doi.org/10.1016/j.matlet.2021.129751.
26. Korkmaz, S.; Kariper, İ.A., Graphene and Graphene Oxide Based Aerogels: Synthesis, Characteristics and Supercapacitor Applications.*J. Energy Storage*, **2020**, *27*, 101038, https://doi.org/10.1016/j.est.2019.101038.
27. Loh, K.P.; Bao, Q.; Eda, G.; Chhowalla, M., Graphene Oxide as a Chemically Tunable Platform for Optical Applications *Nat. Chem.*, **2010**, *2*, 1015–1024, https://doi.org/10.1038/nchem.907.
28. Liu, J.; Cui, L.; Losic, D. Graphene and Graphene Oxide as New Nanocarriers for Drug Delivery Applications.*Acta Biomater.*, **2013**, *9*, 9243–9257, https://doi.org/10.1016/j.actbio.2013.08.016.
29. Shafiee, A.; Iravani, S.; Varma, R.S., Graphene and Graphene Oxide with Anticancer Applications: Challenges and Future Perspectives.*MedComm*, **2022**, *3*, https://doi.org/10.1002/mco2.118.
30. Banoon, S.R.; Ghasemian, A., The Characters of Graphene Oxide Nanoparticles and Doxorubicin Against HCT-116 Colorectal Cancer Cells *In vitro*.*J. Gastrointest. Cancer*, **2022**, *53*, 410–414, https://doi.org/10.1007/s12029-021-00625-x.
31. Wang, Y.; Li, Z.; Wang, J.; Li, J.; Lin, Y., Graphene and Graphene Oxide: Biofunctionalization and Applications in Biotechnology.*Trends Biotechnol.*, **2011**, *29*, 205–212, https://doi.org/10.1016/j.tibtech.2011.01.008.
32. Hasanin, M.; Taha, N.F.; Abdou, A.R.; Emara, L.H., Green Decoration of Graphene Oxide Nano Sheets with Gelatin and Gum Arabic for Targeted Delivery of Doxorubicin.*Biotechnol. Rep.*, **2022**, *34*, e00722, https://doi.org/10.1016/j.btre.2022.e00722.
33. Teniou, A.; Rhouati, A.; Catanante, G., A Simple Fluorescent Aptasensing Platform Based on Graphene Oxide for Dopamine Determination.*Appl. Biochem. Biotechnol.*, **2022**, *194*, 1925–1937, https://doi.org/10.1007/s12010-022-03802-1.
34. Hasanin, M.S.; El-Sakhawy, M.; Ahmed, Hanaa.Y.; Kamel, S., Hydroxypropyl Methylcellulose/Graphene Oxide Composite as Drug Carrier System for 5-fluorouracil.*Biotechnol. J.*, **2022**, *17*, 2100183, https://doi.org/10.1002/biot.202100183.
35. Zhu, Y.; Murali, S.; Cai, W.; Li, X.; Suk, J.W.; Potts, J.R.; Ruoff, R.S. Graphene and Graphene Oxide: Synthesis, Properties, and Applications.*Adv. Mater.*, **2010**, *22*, 3906–3924, https://doi.org/10.1002/adma.201001068.
36. Yue, W.; Liu, C.; Zha, Z.; Liu, R.; Gao, J.; Shafi, M.; Feng, J.; Jiang, S. Composite Substrate of Graphene/Ag Nanoparticles Coupled with a Multilayer Film for Surface-Enhanced Raman Scattering Biosensing.*Opt. Express*, **2022**, *30*, 13226, https://doi.org/10.1364/OE.454893.
37. Tabish, T.A.; Hayat, H.; Abbas, A.; Narayan, R.J., Graphene Quantum Dots-Based Electrochemical Biosensing Platform for Early Detection of Acute Myocardial Infarction.*Biosensors*, **2022**, *12*, 77, https://doi.org/10.3390/bios12020077.
38. Jiang, H. Chemical Preparation of Graphene-Based Nanomaterials and Their Applications in Chemical and Biological Sensors.*Small*, **2011**, n/a-n/a, https://doi.org/10.1002/smll.201002352.
39. Zhou, M.; Zhai, Y.; Dong, S.Electrochemical Sensing and Biosensing Platform Based on Chemically Reduced Graphene Oxide.*Anal. Chem.***2009**, *81*, 5603–5613, https://doi.org/10.1021/ac900136z.
40. Geim, A.K.Graphene: Status and Prospects, *Science*, **2009**, *324*, 1530–1534, https://doi.org/10.1126/science.1158877.

41. XIII. On the Atomic Weight of Graphite.*Philos. Trans. R. Soc. Lond.*, **1859**, *149*, 249–259, https://doi.org/10.1098/rstl.1859.0013.
42. Yusuf, M.; Elfghi, F.M.; Zaidi, S.A.; Abdullah, E.C.; Khan, M.A. Applications of Graphene and Its Derivatives as an Adsorbent for Heavy Metal and Dye Removal: A Systematic and Comprehensive Overview.*RSC Adv.*, **2015**, *5*, 50392–50420, https://doi.org/10.1039/C5RA07223A.
43. Novoselov, K.S.; Geim, A.K.; Morozov, S.V.; Jiang, D.; Zhang, Y.; Dubonos, S.V.; Grigorieva, I.V.; Firsov, A.A., Electric Field Effect in Atomically Thin Carbon Films.*Science*, **2004**, *306*, 666–669, https://doi.org/10.1126/science.1102896.
44. Berger, C.; Song, Z.; Li, X.; Wu, X.; Brown, N.; Naud, C.; Mayou, D.; Li, T.; Hass, J.; Marchenkov, A.N.; Conrad, E.H.; First, P.N.; de Heer, W.A.. Electronic Confinement and Coherence in Patterned Epitaxial Graphene.*Science*, **2006**, *312*, 1191–1196, https://doi.org/10.1126/science.1125925.
45. Choi, W.; Lahiri, I.; Seelaboyina, R.; Kang, Y.S., Synthesis of Graphene and Its Applications: A Review.*Crit. Rev. Solid State Mater. Sci.*, **2010**, *35*, 52–71, https://doi.org/10.1080/10408430903505036.
46. Singh, V.; Joung, D.; Zhai, L.; Das, S.; Khondaker, S.I.; Seal, S., Graphene Based Materials: Past, Present and Future. *Prog. Mater. Sci.*, **2011**, *56*, 1178–1271, https://doi.org/10.1016/j.pmatsci.2011.03.003.
47. Marcano, D.C.; Kosynkin, D.V.; Berlin, J.M.; Sinitskii, A.; Sun, Z.; Slesarev, A.; Alemany, L.B.; Lu, W.; Tour, J.M., Improved Synthesis of Graphene Oxide.*ACS Nano*, **2010**, *4*, 4806–4814, https://doi.org/10.1021/nn1006368.
48. Abdolhosseinzadeh, S.; Asgharzadeh, H.; Seop Kim, H., Fast and Fully-Scalable Synthesis of Reduced Graphene Oxide.*Sci. Rep.*, **2015**, *5*, 10160, https://doi.org/10.1038/srep10160.
49. ~~Toda, K.; Furue, R.; Hayami, S. Recent Progress in Applications of Graphene Oxide for Gas Sensing: A Review.*Anal. Chim. Acta*, **2015**, *878*, 43–53, https://doi.org/10.1016/j.aca.2015.02.002.~~
49. Jiříčková, A.; Jankovský, O.; Sofer, Z.; Sedmidubský, D., Synthesis and Applications of Graphene Oxide, *Materials*, **2022**, *15*, 920, https://doi.org/10.3390/ma15030920.
50. Nandee, R.; Chowdhury, M.A.; Shahid, A.; Hossain, N.; Rana, M. Band Gap Formation of 2D Materialin Graphene: Future Prospect and Challenges.*Results Eng.*, **2022**, *15*, 100474, https://doi.org/10.1016/j.rineng.2022.100474.
51. Wang, B.; Song, C. Graphene Bandgap Opening by Constructing Superlattices with BN or MoO_2 under Pressure.*J. Phys. Conf. Ser.***2022**, *2331*, 012001, https://doi.org/10.1088/1742-6596/2331/1/012001.
52. Novoselov, K.S.; Geim, A.K.; Morozov, S.V.; Jiang, D.; Katsnelson, M.I.; Grigorieva, I.V.; Dubonos, S.V.; Firsov, A.A. Two-Dimensional Gas of Massless Dirac Fermions in Graphene, *Nature*, **2005**, *438*, 197–200, https://doi.org/10.1038/nature04233.
53. Zhang, Y.; Tan, Y.-W.; Stormer, H.L.; Kim, P., Experimental Observation of the Quantum Hall Effect and Berry's Phase in Graphene.*Nature*, **2005**, *438*, 201–204, https://doi.org/10.1038/nature04235.
54. Schedin, F.; Geim, A.K.; Morozov, S.V.; Hill, E.W.; Blake, P.; Katsnelson, M.I.; Novoselov, K.S., Detection of Individual Gas Molecules Adsorbed on Graphene.*Nat. Mater.*, **2007**, *6*, 652–655, https://doi.org/10.1038/nmat1967.
55. Dan, Y.; Lu, Y.; Kybert, N.J.; Luo, Z.; Johnson, A.T.C., Intrinsic Response of Graphene Vapor Sensors.*Nano Lett.*, **2009**, *9*, 1472–1475, https://doi.org/10.1021/nl8033637.
56. Robinson, J.T.; Perkins, F.K.; Snow, E.S.; Wei, Z.; Sheehan, P.E., Reduced Graphene Oxide Molecular Sensors. *Nano Lett.*, **2008**, *8*, 3137–3140, https://doi.org/10.1021/nl8013007.
57. Tang, L.; Wang, Y.; Li, Y.; Feng, H.; Lu, J.; Li, J., Preparation, Structure, and Electrochemical Properties of Reduced Graphene Sheet Films.*Adv. Funct. Mater.*, **2009**, *19*, 2782–2789, https://doi.org/10.1002/adfm.200900377.
58. Ohno, Y.; Maehashi, K.; Yamashiro, Y.; Matsumoto, K., Electrolyte-Gated Graphene Field-Effect Transistors for Detecting PH and Protein Adsorption.*Nano Lett.*, **2009**, *9*, 3318–3322, https://doi.org/10.1021/nl901596m.
59. Mohanty, N.; Berry, V., Graphene-Based Single-Bacterium Resolution Biodevice and DNA Transistor: Interfacing Graphene Derivatives with Nanoscale and Microscale Biocomponents *Nano Lett.*, **2008**, *8*, 4469–4476, https://doi.org/10.1021/nl802412n.
60. Machado, M.; Oliveira, A.M.L.; Silva, G.A.; Bitoque, D.B.; Tavares Ferreira, J.; Pinto, L.A.; Ferreira, Q., Graphene Biosensors—A Molecular Approach.*Nanomaterials*, **2022**, *12*, 1624, https://doi.org/10.3390/nano12101624.
61. Ji, G.; Tian, J.; Xing, F.; Feng, Y., Optical Biosensor Based on Graphene and Its Derivatives for Detecting Biomolecules.*Int. J. Mol. Sci.***2022**, *23*, 10838, https://doi.org/10.3390/ijms231810838.
62. Leenaerts, O.; Partoens, B.; Peeters, F.M., Adsorption of H 2 O , N H 3 , CO, N O 2 , and NO on Graphene: A First-Principles Study.*Phys. Rev. B*, **2008**, *77*, 125416, https://doi.org/10.1103/PhysRevB.77.125416.
63. Das, P.; Das, M.; Chinnadayyala, S.R.; Singha, I.M.; Goswami, P., Recent Advances on Developing 3rd Generation Enzyme Electrode for Biosensor Applications.*Biosens. Bioelectron.*, **2016**, *79*, 386–397, https://doi.org/10.1016/j.bios.2015.12.055.

64. Baghayeri, M.; Zare, E.N.; Namadchian, M., Direct Electrochemistry and Electrocatalysis of Hemoglobin Immobilized on Biocompatible Poly(Styrene-Alternative-Maleic Acid)/Functionalized Multi-Wall Carbon Nanotubes Blends.*Sens. Actuators B Chem.*, **2013**, *188*, 227–234, https://doi.org/10.1016/j.snb.2013.07.028.
65. Luong, J.H.T.; Glennon, J.D.; Gedanken, A.; Vashist, S.K., Achievement and Assessment of Direct Electron Transfer of Glucose Oxidase in Electrochemical Biosensing Using Carbon Nanotubes, Graphene, and Their Nanocomposites.*Microchim. Acta*, **2017**, *184*, 369–388, https://doi.org/10.1007/s00604-016-2049-3.
66. Cipolatti, E.P.; Silva, M.J.A.; Klein, M.; Feddern, V.; Feltes, M.M.C.; Oliveira, J.V.; Ninow, J.L.; de Oliveira, D., Current Status and Trends in Enzymatic Nanoimmobilization.*J. Mol. Catal. B Enzym.*, **2014**, *99*, 56–67, https://doi.org/10.1016/j.molcatb.2013.10.019.
67. Putzbach, W.; Ronkainen, N. Immobilization Techniques in the Fabrication of Nanomaterial-Based Electrochemical Biosensors: A Review.*Sensors***2013**, *13*, 4811–4840, https://doi.org/10.3390/s130404811.
68. Hwang, E.T.; Gu, M.B., Enzyme Stabilization by Nano/Microsized Hybrid Materials: Enzyme Stabilization by Nano/Microsized Hybrid Materials.*Eng. Life Sci.*, **2013**, *13*, 49–61, https://doi.org/10.1002/elsc.201100225.
69. Cipolatti, E.P.; Valério, A.; Henriques, R.O.; Moritz, D.E.; Ninow, J.L.; Freire, D.M.G.; Manoel, E.A.; Fernandez-Lafuente, R.; de Oliveira, D., Nanomaterials for Biocatalyst Immobilization – State of the Art and Future Trends. *RSC Adv.*, **2016**, *6*, 104675–104692, https://doi.org/10.1039/C6RA22047A.
70. Lawal, A.T., Synthesis and Utilisation of Graphene for Fabrication of Electrochemical Sensors. *Talanta*, **2015**, *131*, 424–443, https://doi.org/10.1016/j.talanta.2014.07.019.
71. Shan, C.; Yang, H.; Song, J.; Han, D.; Ivaska, A.; Niu, L., Direct Electrochemistry of Glucose Oxidase and Biosensing for Glucose Based on Graphene.*Anal. Chem.*, **2009**, *81*, 2378–2382, https://doi.org/10.1021/ac802193c.
72. Kang, X.; Wang, J.; Wu, H.; Aksay, I.A.; Liu, J.; Lin, Y. Glucose Oxidase–Graphene–Chitosan Modified Electrode for Direct Electrochemistry and Glucose Sensing.*Biosens. Bioelectron.*, **2009**, *25*, 901–905, https://doi.org/10.1016/j.bios.2009.09.004.
73. Dey, R.S.; Raj, C.R., Development of an Amperometric Cholesterol Biosensor Based on Graphene−Pt Nanoparticle Hybrid Material.*J. Phys. Chem. C*, **2010**, *114*, 21427–21433, https://doi.org/10.1021/jp105895a.
74. He, Y.; Sheng, Q.; Zheng, J.; Wang, M.; Liu, B. Magnetite–Graphene for the Direct Electrochemistry of Hemoglobin and Its Biosensing Application.*Electrochimica Acta*, **2011**, *56*, 2471–2476, https://doi.org/10.1016/j.electacta.2010.11.020.
75. Wu, J.-F.; Xu, M.-Q.; Zhao, G.-C., Graphene-Based Modified Electrode for the Direct Electron Transfer of Cytochrome c and Biosensing.*Electrochem. Commun.*, **2010**, *12*, 175–177, https://doi.org/10.1016/j.elecom.2009.11.020.
76. Dey, R.S.; Raj, C.R., Redox-Functionalized Graphene Oxide Architecture for the Development of Amperometric Biosensing Platform. *ACS Appl. Mater. Interfaces*, **2013**, *5*, 4791–4798, https://doi.org/10.1021/am400280u.
77. Xu, H.; Wang, D.; He, S.; Li, J.; Feng, B.; Ma, P.; Xu, P.; Gao, S.; Zhang, S.; Liu, Q.; Lu, J.; Song, S.; Fan, C., Graphene-Based Nanoprobes and a Prototype Optical Biosensing Platform.*Biosens. Bioelectron.*, **2013**, *50*, 251–255, https://doi.org/10.1016/j.bios.2013.06.039.
78. Anik, Ü., Gold Nanoparticle-Based Electrochemical Biosensors for Medical Applications. In: *Biomedical Materials and Diagnostic Devices*; Tiwari, A.; Ramalingam, M.; Kobayashi, H.; Turner, A.P.F., Eds.; John Wiley & Sons, Inc.: Hoboken, NJ, USA, **2012**; pp. 263–277, https://doi.org/10.1002/9781118523025.ch8.
79. Matsumoto, K.; Maehashi, K.; Ohno, Y.; Inoue, K., Recent Advances in Functional Graphene Biosensors. *J. Phys. Appl. Phys.*, **2014**, *47*, 094005, https://doi.org/10.1088/0022-3727/47/9/094005.
80. Cheng, S.; Tang, D.; Zhang, Y.; Xu, L.; Liu, K.; Huang, K.; Yin, Z., Specific and Sensitive Detection of Tartrazine on the Electrochemical Interface of a Molecularly Imprinted Polydopamine-Coated PtCo Nanoalloy on Graphene Oxide.*Biosensors*, **2022**, *12*, 326, https://doi.org/10.3390/bios12050326.
81. Işın, D.; Eksin, E.; Erdem, A., Graphene-Oxide and Ionic Liquid Modified Electrodes for Electrochemical Sensing of Breast Cancer 1 Gene. *Biosensors*, **2022**, *12*, 95, https://doi.org/10.3390/bios12020095.
82. Parnianchi, F.; Nazari, M.; Maleki, J.; Mohebi, M., Combination of Graphene and Graphene Oxide with Metal and Metal Oxide Nanoparticles in Fabrication of Electrochemical Enzymatic Biosensors.*Int. Nano Lett.*, **2018**, *8*, 229–239, https://doi.org/10.1007/s40089-018-0253-3.
83. Zhou, K.; Zhu, Y.; Yang, X.; Luo, J.; Li, C.; Luan, S., A Novel Hydrogen Peroxide Biosensor Based on Au–Graphene–HRP–Chitosan Biocomposites. *Electrochimica Acta*, **2010**, *55*, 3055–3060, https://doi.org/10.1016/j.electacta.2010.01.035.
84. Sheng, Q.; Wang, M.; Zheng, J., A Novel Hydrogen Peroxide Biosensor Based on Enzymatically Induced Deposition of Polyaniline on the Functionalized Graphene–Carbon Nanotube Hybrid Materials.*Sens. Actuators B Chem.*, **2011**, *160*, 1070–1077, https://doi.org/10.1016/j.snb.2011.09.028.
85. Cheng, J.; Zhang, M.; Wu, G.; Wang, X.; Zhou, J.; Cen, K. Photoelectrocatalytic Reduction of CO_2 into Chemicals Using Pt-Modified Reduced Graphene Oxide Combined with Pt-Modified TiO_2 Nanotubes.*Environ. Sci. Technol.*, **2014**, *48*, 7076–7084, https://doi.org/10.1021/es500364g.

86. Shan, C.; Yang, H.; Han, D.; Zhang, Q.; Ivaska, A.; Niu, L., Graphene/AuNPs/Chitosan Nanocomposites Film for Glucose Biosensing.*Biosens. Bioelectron.*, **2010**, *25*, 1070–1074, https://doi.org/10.1016/j.bios.2009.09.024.
87. Pan, D.; Gu, Y.; Lan, H.; Sun, Y.; Gao, H., Functional Graphene-Gold Nano-Composite Fabricated Electrochemical Biosensor for Direct and Rapid Detection of Bisphenol A.*Anal. Chim. Acta*, **2015**, *853*, 297–302, https://doi.org/10.1016/j.aca.2014.11.004.
88. Shen, M.; Wu, C.; Lin, C.; Fan, G.; Jin, Y.; Zhang, Z.; Li, C.; Jia, W. FACILE SOLVOTHERMAL SYNTHESIS OF MESOSTRUCTURED CHITOSAN-COATED Fe $_3$ O $_4$ NANOPARTICLES AND ITS FURTHER MODIFICATION WITH FOLIC ACID FOR IMPROVING TARGETED DRUG DELIVERY.*Nano*, **2014**, *09*, 1450081, https://doi.org/10.1142/S1793292014500817.
89. Xu, Q.; Gu, S.-X.; Jin, L.; Zhou, Y.; Yang, Z.; Wang, W.; Hu, X. Graphene/Polyaniline/Gold Nanoparticles Nanocomposite for the Direct Electron Transfer of Glucose Oxidase and Glucose Biosensing.*Sens. Actuators B Chem.*, **2014**, *190*, 562–569, https://doi.org/10.1016/j.snb.2013.09.049.
90. Sun, J.-Y.; Huang, K.-J.; Zhao, S.-F.; Fan, Y.; Wu, Z.-W. Direct Electrochemistry and Electrocatalysis of Hemoglobin on Chitosan-Room Temperature Ionic Liquid-TiO2-Graphene Nanocomposite Film Modified Electrode.*Bioelectrochemistry*, **2011**, *82*, 125–130, https://doi.org/10.1016/j.bioelechem.2011.06.007.
91. Wang, J.T.-W.; Ball, J.M.; Barea, E.M.; Abate, A.; Alexander-Webber, J.A.; Huang, J.; Saliba, M.; Mora-Sero, I.; Bisquert, J.; Snaith, H.J.; Nicholas, R.J., Low-Temperature Processed Electron Collection Layers of Graphene/TiO $_2$ Nanocomposites in Thin Film Perovskite Solar Cells.*Nano Lett.*, **2014**, *14*, 724–730, https://doi.org/10.1021/nl403997a.
92. Xin, Y.; Fu-bing, X.; Hong-wei, L.; Feng, W.; Di-zhao, C.; Zhao-yang, W., A Novel H2O2 Biosensor Based on Fe3O4–Au Magnetic Nanoparticles Coated Horseradish Peroxidase and Graphene Sheets–Nafion Film Modified Screen-Printed Carbon Electrode.*Electrochimica Acta*, **2013**, *109*, 750–755, https://doi.org/10.1016/j.electacta.2013.08.011.
93. Zhu, S.; Guo, J.; Dong, J.; Cui, Z.; Lu, T.; Zhu, C.; Zhang, D.; Ma, J. Sonochemical Fabrication of Fe3O4 Nanoparticles on Reduced Graphene Oxide for Biosensors.*Ultrason. Sonochem.*, **2013**, *20*, 872–880, https://doi.org/10.1016/j.ultsonch.2012.12.001.
94. Sun, W.; Gong, S.; Deng, Y.; Li, T.; Cheng, Y.; Wang, W.; Wang, L., Electrodeposited Nickel Oxide and Graphene Modified Carbon Ionic Liquid Electrode for Electrochemical Myglobin Biosensor.*Thin Solid Films*, **2014**, *562*, 653–658, https://doi.org/10.1016/j.tsf.2014.05.002.
95. Xia, S.-Y.; Long, Y.; Huang, Z.; Zi, Y.; Tao, L.-Q.; Li, C.-H.; Sun, H.; Li, J. Laser-Induced Graphene (LIG)-Based Pressure Sensor and Triboelectric Nanogenerator towards High-Performance Self-Powered Measurement-Control Combined System.*Nano Energy*, **2022**, *96*, 107099, https://doi.org/10.1016/j.nanoen.2022.107099.
96. Yang, Y.; Shen, H.; Yang, Z.; Yang, J.; Wang, Z.; Gao, K., Highly Flexible and Sensitive Wearable Strain and Pressure Sensor Based on Porous Graphene Paper for Human Motion.*J. Mater. Sci. Mater. Electron.*, **2022**, *33*, 17637–17648, https://doi.org/10.1007/s10854-022-08627-6.
97. Boland, C.S.; Khan, U.; Backes, C.; O'Neill, A.; McCauley, J.; Duane, S.; Shanker, R.; Liu, Y.; Jurewicz, I.; Dalton, A.B.; Coleman, J.N., Sensitive, High-Strain, High-Rate Bodily Motion Sensors Based on Graphene–Rubber Composites.*ACS Nano*, **2014**, *8*, 8819–8830, https://doi.org/10.1021/nn503454h.
98. Hempel, M.; Nezich, D.; Kong, J.; Hofmann, M., A Novel Class of Strain Gauges Based on Layered Percolative Films of 2D Materials.*Nano Lett.***2012**, *12*, 5714–5718, https://doi.org/10.1021/nl302959a.
99. Bae, S.-H.; Lee, Y.; Sharma, B.K.; Lee, H.-J.; Kim, J.-H.; Ahn, J.-H., Graphene-Based Transparent Strain Sensor.*Carbon*, **2013**, *51*, 236–242, https://doi.org/10.1016/j.carbon.2012.08.048.
100. Tian, H.; Shu, Y.; Cui, Y.-L.; Mi, W.-T.; Yang, Y.; Xie, D.; Ren, T.-L., Scalable Fabrication of High-Performance and Flexible Graphene Strain Sensors. *Nanoscale*, **2014**, *6*, 699–705, https://doi.org/10.1039/C3NR04521H.
101. Xu, W.; Yang, T.; Qin, F.; Gong, D.; Du, Y.; Dai, G., A Sprayed Graphene Pattern-Based Flexible Strain Sensor with High Sensitivity and Fast Response, *Sensors*, **2019**, *19*, 1077, https://doi.org/10.3390/s19051077.
102. Irani, F.S.; Shafaghi, A.H.; Tasdelen, M.C.; Delipinar, T.; Kaya, C.E.; Yapici, G.G.; Yapici, M.K., Graphene as a Piezoresistive Material in Strain Sensing Applications.*Micromachines*, **2022**, *13*, 119, https://doi.org/10.3390/mi13010119.
103. Patole, S.P.; Reddy, S.K.; Schiffer, A.; Askar, K.; Prusty, B.G.; Kumar, S., Piezoresistive and Mechanical Characteristics of Graphene Foam Nanocomposites.*ACS Appl. Nano Mater.*, **2019**, *2*, 1402–1411, https://doi.org/10.1021/acsanm.8b02306.
104. Gong, T.; Zhang, H.; Huang, W.; Mao, L.; Ke, Y.; Gao, M.; Yu, B. Highly Responsive Flexible Strain Sensor Using Polystyrene Nanoparticle Doped Reduced Graphene Oxide for Human Health Monitoring.*Carbon*, **2018**, *140*, 286–295, https://doi.org/10.1016/j.carbon.2018.09.007.
105. Li, X.; Zhang, R.; Yu, W.; Wang, K.; Wei, J.; Wu, D.; Cao, A.; Li, Z.; Cheng, Y.; Zheng, Q.; Ruoff, R.S.; Zhu, H., Stretchable and Highly Sensitive Graphene-on-Polymer Strain Sensors. *Sci. Rep.*, **2012**, *2*, 870, https://doi.org/10.1038/srep00870.

106. Xu, Y.; Guo, Z.; Chen, H.; Yuan, Y.; Lou, J.; Lin, X.; Gao, H.; Chen, H.; Yu, B., In-Plane and Tunneling Pressure Sensors Based on Graphene/Hexagonal Boron Nitride Heterostructures.*Appl. Phys. Lett.*, **2011**, *99*, 133109, https://doi.org/10.1063/1.3643899.
107. Trung, T.Q.; Lee, N.-E., Flexible and Stretchable Physical Sensor Integrated Platforms for Wearable Human-Activity Monitoringand Personal Healthcare.*Adv. Mater.*, **2016**, *28*, 4338–4372, https://doi.org/10.1002/adma.201504244.
108. Ryu, S.; Lee, P.; Chou, J.B.; Xu, R.; Zhao, R.; Hart, A.J.; Kim, S.-G., Extremely Elastic Wearable Carbon Nanotube Fiber Strain Sensor for Monitoring of Human Motion. *ACS Nano*, **2015**, *9*, 5929–5936, https://doi.org/10.1021/acsnano.5b00599.
109. Viventi, J.; Kim, D.-H.; Moss, J.D.; Kim, Y.-S.; Blanco, J.A.; Annetta, N.; Hicks, A.; Xiao, J.; Huang, Y.; Callans, D.J.; Rogers, J.A.; Litt, B., A Conformal, Bio-Interfaced Class of Silicon Electronics for Mapping Cardiac Electrophysiology.*Sci. Transl. Med.*, **2010**, *2*, https://doi.org/10.1126/scitranslmed.3000738.
110. Chang, N.-K.; Su, C.-C.; Chang, S.-H. Fabrication of Single-Walled Carbon Nanotube Flexible Strain Sensors with High Sensitivity.*Appl. Phys. Lett.*, **2008**, *92*, 063501, https://doi.org/10.1063/1.2841669.
111. Lipomi, D.J.; Vosgueritchian, M.; Tee, B.C.-K.; Hellstrom, S.L.; Lee, J.A.; Fox, C.H.; Bao, Z., Skin-like Pressure and Strain Sensors Based on Transparent Elastic Films of Carbon Nanotubes.*Nat. Nanotechnol*.**2011**, *6*, 788–792, https://doi.org/10.1038/nnano.2011.184.
112. Zhou, J.; Yu, H.; Xu, X.; Han, F.; Lubineau, G., Ultrasensitive, Stretchable Strain Sensors Based on Fragmented Carbon Nanotube Papers.*ACS Appl. Mater. Interfaces*, **2017**, *9*, 4835–4842, https://doi.org/10.1021/acsami.6b15195.
113. Wang, Y.; Yang, T.; Lao, J.; Zhang, R.; Zhang, Y.; Zhu, M.; Li, X.; Zang, X.; Wang, K.; Yu, W.; Jin, H.; Wang, L.; Zhu, H., Ultra-Sensitive Graphene Strain Sensor for Sound Signal Acquisition and Recognition.*Nano Res.*, **2015**, *8*, 1627–1636, https://doi.org/10.1007/s12274-014-0652-3.
114. Li, X.; Sun, P.; Fan, L.; Zhu, M.; Wang, K.; Zhong, M.; Wei, J.; Wu, D.; Cheng, Y.; Zhu, H., Multifunctional Graphene Woven Fabrics.*Sci. Rep.*, **2012**, *2*, 395, https://doi.org/10.1038/srep00395.
115. Yan, C.; Wang, J.; Kang, W.; Cui, M.; Wang, X.; Foo, C.Y.; Chee, K.J.; Lee, P.S. Highly Stretchable Piezoresistive Graphene-Nanocellulose Nanopaper for Strain Sensors.*Adv. Mater.*, **2014**, *26*, 2022–2027, https://doi.org/10.1002/adma.201304742.
116. Sánchez, M.F.; Els-Heindl, S.; Beck-Sickinger, A.G.; Wieneke, R.; Tampé, R., Photoinduced Receptor Confinement Drives Ligand-Independent GPCR Signaling.*Science*, **2021**, *371*, eabb7657, https://doi.org/10.1126/science.abb7657.
117. Wang, Y.; Wang, L.; Yang, T.; Li, X.; Zang, X.; Zhu, M.; Wang, K.; Wu, D.; Zhu, H., Wearable and Highly Sensitive Graphene Strain Sensors for Human Motion Monitoring.*Adv. Funct. Mater.*, **2014**, *24*, 4666–4670, https://doi.org/10.1002/adfm.201400379.
118. Hontoria-Lucas, C.; López-Peinado, A.J.; López-González, J. de D.; Rojas-Cervantes, M.L.; Martín-Aranda, R.M., Study of Oxygen-Containing Groups in a Series of Graphite Oxides: Physical and Chemical Characterization.*Carbon*, **1995**, *33*, 1585–1592, https://doi.org/10.1016/0008-6223(95)00120-3.
119. Szabó, T.; Tombácz, E.; Illés, E.; Dékány, I., Enhanced Acidity and PH-Dependent Surface Charge Characterization of Successively Oxidized Graphite Oxides.*Carbon*, **2006**, *44*, 537–545, https://doi.org/10.1016/j.carbon.2005.08.005.
120. Cassagneau, T.; Guérin, F.; Fendler, J.H., Preparation and Characterization of Ultrathin Films Layer-by-Layer Self-Assembled from Graphite Oxide Nanoplatelets and Polymers.*Langmuir*, **2000**, *16*, 7318–7324, https://doi.org/10.1021/la000442o.
121. Jeong, H.-K.; Lee, Y.P.; Lahaye, R.J.W.E.; Park, M.-H.; An, K.H.; Kim, I.J.; Yang, C.-W.; Park, C.Y.; Ruoff, R.S.; Lee, Y.H., Evidence of Graphitic AB Stacking Order of Graphite Oxides. *J. Am. Chem. Soc.*, **2008**, *130*, 1362–1366, https://doi.org/10.1021/ja076473o.
122. Rigoletto, M.; Calza, P.; Gaggero, E.; Laurenti, E., Hybrid Materials for the Removal of Emerging Pollutants in Water: Classification, Synthesis, and Properties.*Chem. Eng. J. Adv.*, **2022**, *10*, 100252, https://doi.org/10.1016/j.ceja.2022.100252.
123. Chi, H.; Liu, Y.J.; Wang, F.; He, C., Highly Sensitive and Fast Response Colorimetric Humidity Sensors Based on Graphene Oxides Film, *ACS Appl. Mater. Interfaces*, **2015**, *7*, 19882–19886, https://doi.org/10.1021/acsami.5b06883.
124. An, J.; Le, T.-S.D.; Huang, Y.; Zhan, Z.; Li, Y.; Zheng, L.; Huang, W.; Sun, G.; Kim, Y.-J., All-Graphene-Based Highly Flexible Noncontact Electronic Skin, *ACS Appl. Mater. Interfaces*, **2017**, *9*, 44593–44601, https://doi.org/10.1021/acsami.7b13701.
125. Kim, Y.H.; Kim, S.J.; Kim, Y.-J.; Shim, Y.-S.; Kim, S.Y.; Hong, B.H.; Jang, H.W., Self-Activated Transparent All-Graphene Gas Sensor with Endurance to Humidity and Mechanical Bending, *ACS Nano*, **2015**, *9*, 10453–10460, https://doi.org/10.1021/acsnano.5b04680.
126. Qiao, Y.; Li, X.; Hirtz, T.; Deng, G.; Wei, Y.; Li, M.; Ji, S.; Wu, Q.; Jian, J.; Wu, F.; Shen, Y.; Tian, H.; Yang, Y.; Ren, T.-L. Graphene-Based Wearable Sensors. *Nanoscale*, **2019**, *11*, 18923–18945, https://doi.org/10.1039/C9NR05532K.

127. Gupta Chatterjee, S.; Chatterjee, S.; Ray, A.K.; Chakraborty, A.K., Graphene–Metal Oxide Nanohybrids for Toxic Gas Sensor: A Review.*Sens. Actuators B Chem.*, **2015**, *221*, 1170–1181, https://doi.org/10.1016/j.snb.2015.07.070.
128. Norizan, M.N.; Abdullah, N.; Halim, N.A.; Demon, S.Z.N.; Mohamad, I.S., Heterojunctions of RGO/Metal Oxide Nanocomposites as Promising Gas-Sensing Materials—A Review.*Nanomaterials*, **2022**, *12*, 2278, https://doi.org/10.3390/nano12132278.
129. Timmer, B.; Olthuis, W.; Berg, A. van den, Ammonia Sensors and Their Applications—a Review.*Sens. Actuators B Chem.*, **2005**, *107*, 666–677, https://doi.org/10.1016/j.snb.2004.11.054.
130. Becker, T.; Mühlberger, S.; Braunmühl, Chr.B.; Müller, G.; Ziemann, T.; Hechtenberg, K.V., Air Pollution Monitoring Using Tin-Oxide-Based Microreactor Systems. *Sens. Actuators B Chem.*, **2000**, *69*, 108–119, https://doi.org/10.1016/S0925-4005(00)00516-5.
131. Sutton, M.A.; Erisman, J.W.; Dentener, F.; Möller, D., Ammonia in the Environment: From Ancient Times to the Present. *Environ. Pollut.*, **2008**, *156*, 583–604, https://doi.org/10.1016/j.envpol.2008.03.013.
132. Helmers, S.; Top, F.H.; Knapp, L.W.Ammonia Injuries in Agriculture.*J. Iowa Med. Soc.*, **1971**, *61*, 271–280, https://pubmed.ncbi.nlm.nih.gov/5556686/.
133. Ponzoni, A.; Baratto, C.; Cattabiani, N.; Falasconi, M.; Galstyan, V.; Nunez-Carmona, E.; Rigoni, F.; Sberveglieri, V.; Zambotti, G.; Zappa, D., Metal Oxide Gas Sensors, a Survey of Selectivity Issues Addressed at the SENSOR Lab, Brescia (Italy).*Sensors*, **2017**, *17*, 714, https://doi.org/10.3390/s17040714.
134. Huang, X.-J.; Choi, Y.-K., Chemical Sensors Based on Nanostructured Materials. *Sens. Actuators B Chem.*, **2007**, *122*, 659–671, https://doi.org/10.1016/j.snb.2006.06.022.
135. Qian, H.; Deng, J.; Zhou, H.; Yang, X.; Chen, W., First-Principles Study of Pd-$MoSe_2$ as Sensing Material for Characteristic SF_6 Decomposition Components.*AIP Adv.*, **2019**, *9*, 125013, https://doi.org/10.1063/1.5128831.
136. Miller, D.R.; Akbar, S.A.; Morris, P.A., Nanoscale Metal Oxide-Based Heterojunctions for Gas Sensing: A Review, *Sens. Actuators B Chem.***2014**, *204*, 250–272, https://doi.org/10.1016/j.snb.2014.07.074.
137. Garg, R.; Kumar, V.; Kumar, D.; Chakarvarti, S.K., Polypyrrole Microwires as Toxic Gas Sensors for Ammonia and Hydrogen Sulphide.*J. Sens. Instrum.*, **2015**, *3*, 1–13, https://doi.org/10.7726/jsi.2015.1001.
138. Zhang, D.; Fan, X.; Hao, X.; Dong, G., Facile Fabrication of Polyaniline Nanocapsule Modified Zinc Oxide Hexagonal Microdiscs for H_2S Gas Sensing Applications.*Ind. Eng. Chem. Res.*, **2019**, *58*, 1906–1913, https://doi.org/10.1021/acs.iecr.8b04869.
139. Asad, M.; Sheikhi, M.H.; Pourfath, M.; Moradi, M., High Sensitive and Selective Flexible H2S Gas Sensors Based on Cu Nanoparticle Decorated SWCNTs. *Sens. Actuators B Chem.*, **2015**, *210*, 1–8, https://doi.org/10.1016/j.snb.2014.12.086.
140. Park, S.; Park, C.; Yoon, H., Chemo-Electrical Gas Sensors Based on Conducting Polymer Hybrids. *Polymers*, **2017**, *9*, 155, https://doi.org/10.3390/polym9050155.
141. Zhang, D.; Wu, Z.; Zong, X.; Zhang, Y., Fabrication of Polypyrrole/Zn2SnO4 Nanofilm for Ultra-Highly Sensitive Ammonia Sensing Application.*Sens. Actuators B Chem.*, **2018**, *274*, 575–586, https://doi.org/10.1016/j.snb.2018.08.001.
142. Cui, S.; Pu, H.; Lu, G.; Wen, Z.; Mattson, E.C.; Hirschmugl, C.; Gajdardziska-Josifovska, M.; Weinert, M.; Chen, J., Fast and Selective Room-Temperature Ammonia Sensors Using Silver Nanocrystal-Functionalized Carbon Nanotubes.*ACS Appl. Mater. Interfaces*, **2012**, *4*, 4898–4904, https://doi.org/10.1021/am301229w.
143. Camilli, L.; Passacantando, M. Advances on Sensors Based on Carbon Nanotubes.*Chemosensors*, **2018**, *6*, 62, https://doi.org/10.3390/chemosensors6040062.
144. Tang, S.; Cao, Z.Adsorption and Dissociation of Ammonia on Graphene Oxides: A First-Principles Study.*J. Phys. Chem. C*, **2012**, *116*, 8778–8791, https://doi.org/10.1021/jp212218w.
145. Kumar, R.; Kumar, A.; Singh, R.; kashyap, R.; Kumar, R.; Kumar, D.; Sharma, S.K.; Kumar, M., Room Temperature Ammonia Gas Sensor Using Meta Toluic Acid Functionalized Graphene Oxide.*Mater. Chem. Phys.***2020**, *240*, 121922, https://doi.org/10.1016/j.matchemphys.2019.121922.
146. Zhang, J.; Liu, X.; Neri, G.; Pinna, N., Nanostructured Materials for Room-Temperature Gas Sensors.*Adv. Mater.*, **2016**, *28*, 795–831, https://doi.org/10.1002/adma.201503825.
147. Röck, F.; Barsan, N.; Weimar, U., Electronic Nose: Current Status and Future Trends.*Chem. Rev.*, **2008**, *108*, 705–725, https://doi.org/10.1021/cr068121q.
148. Lupan, O.; Chai, G.; Chow, L., Novel Hydrogen Gas Sensor Based on Single ZnO Nanorod.*Microelectron. Eng.*, **2008**, *85*, 2220–2225, https://doi.org/10.1016/j.mee.2008.06.021.
149. Tharsika, T.; Haseeb, A.S.M.A.; Akbar, S.A.; Sabri, M.F.M. Catalyst Free Single-Step Fabrication of SnO2/ZnO Core–Shell Nanostructures.*Ceram. Int.*, **2014**, *40*, 7601–7605, https://doi.org/10.1016/j.ceramint.2013.11.124.
150. Lupan, O.; Chai, G.; Chow, L., Fabrication of ZnO Nanorod-Based Hydrogen Gas Nanosensor.*Microelectron. J.*, **2007**, *38*, 1211–1216, https://doi.org/10.1016/j.mejo.2007.09.004.
151. Lupan, O.; Chow, L.; Chai, G., A Single ZnO Tetrapod-Based Sensor.*Sens. Actuators B Chem.*, **2009**, *141*, 511–517, https://doi.org/10.1016/j.snb.2009.07.011.

152. Celebi, K.; Buchheim, J.; Wyss, R.M.; Droudian, A.; Gasser, P.; Shorubalko, I.; Kye, J.-I.; Lee, C.; Park, H.G., Ultimate Permeation Across Atomically Thin Porous Graphene. *Science*, **2014**, *344*, 289–292, https://doi.org/10.1126/science.1249097.
153. Kim, H.W.; Yoon, H.W.; Yoon, S.-M.; Yoo, B.M.; Ahn, B.K.; Cho, Y.H.; Shin, H.J.; Yang, H.; Paik, U.; Kwon, S.; Choi, J.-Y.; Park, H.B., Selective Gas Transport Through Few-Layered Graphene and Graphene Oxide Membranes.*Science***2013**, *342*, 91–95, https://doi.org/10.1126/science.1236098.
154. Nair, R.R.; Wu, H.A.; Jayaram, P.N.; Grigorieva, I.V.; Geim, A.K., Unimpeded Permeation of Water Through Helium-Leak–Tight Graphene-Based Membranes.*Science*, **2012**, *335*, 442–444, https://doi.org/10.1126/science.1211694.
155. O'Hern, S.C.; Boutilier, M.S.H.; Idrobo, J.-C.; Song, Y.; Kong, J.; Laoui, T.; Atieh, M.; Karnik, R., Selective Ionic Transport through Tunable Subnanometer Pores in Single-Layer Graphene Membranes.*Nano Lett.*, **2014**, *14*, 1234–1241, https://doi.org/10.1021/nl404118f.
156. Koenig, S.P.; Wang, L.; Pellegrino, J.; Bunch, J.S., Selective Molecular Sieving through Porous Graphene.*Nat. Nanotechnol.*, **2012**, *7*, 728–732, https://doi.org/10.1038/nnano.2012.162.
157. Zhang, X.; Sun, J.; Tang, K.; Wang, H.; Chen, T.; Jiang, K.; Zhou, T.; Quan, H.; Guo, R., Ultralow Detection Limit and Ultrafast Response/Recovery of the H2 Gas Sensor Based on Pd-Doped RGO/ZnO-SnO2 from Hydrothermal Synthesis.*Microsyst. Nanoeng.*, **2022**, *8*, 67, https://doi.org/10.1038/s41378-022-00398-8.
158. Zhang, X.; Liu, Y.; Li, S.; Kong, L.; Liu, H.; Li, Y.; Han, W.; Yeung, K.L.; Zhu, W.; Yang, W.; Qiu, J., New Membrane Architecture with High Performance: ZIF-8 Membrane Supported on Vertically Aligned ZnO Nanorods for Gas Permeation and Separation.*Chem. Mater.*, **2014**, *26*, 1975–1981, https://doi.org/10.1021/cm500269e.
159. Joshi, R.K.; Alwarappan, S.; Yoshimura, M.; Sahajwalla, V.; Nishina, Y., Graphene Oxide: The New Membrane Material. *Appl. Mater. Today*, **2015**, *1*, 1–12, https://doi.org/10.1016/j.apmt.2015.06.002.
160. Rasch, F.; Postica, V.; Schütt, F.; Mishra, Y.K.; Nia, A.S.; Lohe, M.R.; Feng, X.; Adelung, R.; Lupan, O., Highly Selective and Ultra-Low Power Consumption Metal Oxide Based Hydrogen Gas Sensor Employing Graphene Oxide as Molecular Sieve. *Sens. Actuators B Chem.*, **2020**, *320*, 128363, https://doi.org/10.1016/j.snb.2020.128363.
161. Pustelny, T.; Drewniak, S.; Setkiewicz, M.; Maciak, E.; Urbańczyk, M.; Procek, M.; Gut, K.; Opilski, Z.; Jagiello, J.; Lipinska, L., The Sensitivity of Sensor Structures with Oxide Graphene Exposed to Selected Gaseous Atmospheres.*Bull. Pol. Acad. Sci. Tech. Sci.*, **2013**, *61*, 705–710, https://doi.org/10.2478/bpasts-2013-0075.
162. Duan, P.; Duan, Q.; Peng, Q.; Jin, K.; Sun, J. Design of Ultrasensitive Gas Sensor Based on Self-Assembled Pd-SnO2/RGO Porous Ternary Nanocomposites for Ppb-Level Hydrogen.*Sens. Actuators B Chem.*, **2022**, *369*, 132280, https://doi.org/10.1016/j.snb.2022.132280.
163. Wang, B.; Sun, L.; Schneider-Ramelow, M.; Lang, K.-D.; Ngo, H.-D., Recent Advances and Challenges of Nanomaterials-Based Hydrogen Sensors, *Micromachines*, **2021**, *12*, 1429, https://doi.org/10.3390/mi12111429.
164. Anand, K.; Singh, O.; Singh, M.P.; Kaur, J.; Singh, R.C. Hydrogen Sensor Based on Graphene/ZnO Nanocomposite, *Sens. Actuators B Chem.*, **2014**, *195*, 409–415, https://doi.org/10.1016/j.snb.2014.01.029.
165. Das, S.; Roy, S.; Bhattacharya, T.S.; Sarkar, C.K. Efficient Room Temperature Hydrogen Gas Sensor Using ZnO Nanoparticles-Reduced Graphene Oxide Nanohybrid.*IEEE Sens. J.*, **2021**, *21*, 1264–1272, https://doi.org/10.1109/JSEN.2020.3020755.
166. Galstyan, V.; Comini, E.; Kholmanov, I.; Faglia, G.; Sberveglieri, G., Reduced Graphene Oxide/ZnO Nanocomposite for Application in Chemical Gas Sensors.*RSC Adv.*, **2016**, *6*, 34225–34232, https://doi.org/10.1039/C6RA01913G.
167. Pal, P.; Yadav, A.; Chauhan, P.S.; Parida, P.K.; Gupta, A., Reduced Graphene Oxide Based Hybrid Functionalized Films for Hydrogen Detection: Theoretical and Experimental Studies.*Sens. Int.*, **2021**, *2*, 100072, https://doi.org/10.1016/j.sintl.2020.100072.
168. Drmosh, Q.A.; Yamani, Z.H.; Hendi, A.H.; Gondal, M.A.; Moqbel, R.A.; Saleh, T.A.; Khan, M.Y., A Novel Approach to Fabricating a Ternary RGO/ZnO/Pt System for High-Performance Hydrogen Sensor at Low Operating Temperatures.*Appl. Surf. Sci.*, **2019**, *464*, 616–626, https://doi.org/10.1016/j.apsusc.2018.09.128.
169. Ren, H.; Gu, C.; Joo, S.W.; Cui, J.; Sun, Y.; Huang, J. Preparation of SnO_2 Nanorods on Reduced Graphene Oxide and Sensing Properties of as-Grown Nanocomposites towards Hydrogen at Low Working Temperature. *Mater. Express*, **2018**, *8*, 263–271, https://doi.org/10.1166/mex.2018.1428.
170. Dhall, S.; Kumar, M.; Bhatnagar, M.; Mehta, B.R., Dual Gas Sensing Properties of Graphene-Pd/SnO2 Composites for H2 and Ethanol: Role of Nanoparticles-Graphene Interface.*Int. J. Hydrog. Energy*, **2018**, *43*, 17921–17927, https://doi.org/10.1016/j.ijhydene.2018.07.066.
171. Bhati, V.S.; Ranwa, S.; Rajamani, S.; Kumari, K.; Raliya, R.; Biswas, P.; Kumar, M., Improved Sensitivity with Low Limit of Detection of a Hydrogen Gas Sensor Based on RGO-Loaded Ni-Doped ZnO Nanostructures.*ACS Appl. Mater. Interfaces*, **2018**, *10*, 11116–11124, https://doi.org/10.1021/acsami.7b17877.

172. Zhang, D.; Yin, N.; Jiang, C.; Xia, B., Characterization of CuO–Reduced Graphene Oxide Sandwiched Nanostructure and Its Hydrogen Sensing Characteristics.*J. Mater. Sci. Mater. Electron.*, **2017**, *28*, 2763–2768, https://doi.org/10.1007/s10854-016-5856-8.
173. Dutta, D.; Hazra, S.K.; Das, J.; Sarkar, C.K.; Basu, S., Studies on P-TiO2/n-Graphene Heterojunction for Hydrogen Detection.*Sens. Actuators B Chem.*, **2015**, *212*, 84–92, https://doi.org/10.1016/j.snb.2015.02.009.
174. Venkatesan, A.; Rathi, S.; Lee, I.; Park, J.; Lim, D.; Kang, M.; Joh, H.-I.; Kim, G.-H.; Kannan, E.S., Molybdenum Disulfide Nanoparticles Decorated Reduced Graphene Oxide: Highly Sensitive and Selective Hydrogen Sensor.*Nanotechnology*, **2017**, *28*, 365501, https://doi.org/10.1088/1361-6528/aa7d66.
175. Peng, Y.; Zheng, L.; Zou, K.; Li, C., Enhancing Performances of a Resistivity-Type Hydrogen Sensor Based on Pd/SnO $_2$ /RGO Nanocomposites.*Nanotechnology*, **2017**, *28*, 215501, https://doi.org/10.1088/1361-6528/aa6a96.
176. Venkatesan, A.; Rathi, S.; Lee, I.-Y.; Park, J.; Lim, D.; Kim, G.-H.; Kannan, E.S., Low Temperature Hydrogen Sensing Using Reduced Graphene Oxide and Tin Oxide Nanoflowers Based Hybrid Structure.*Semicond. Sci. Technol.*, **2016**, *31*, 125014, https://doi.org/10.1088/0268-1242/31/12/125014.
177. Esfandiar, A.; Irajizad, A.; Akhavan, O.; Ghasemi, S.; Gholami, M.R., Pd–WO3/Reduced Graphene Oxide Hierarchical Nanostructures as Efficient Hydrogen Gas Sensors.*Int. J. Hydrog. Energy*, **2014**, *39*, 8169–8179, https://doi.org/10.1016/j.ijhydene.2014.03.117.
178. Wang, Y.; Liu, L.; Sun, F.; Li, T.; Zhang, T.; Qin, S., Humidity-Insensitive NO2 Sensors Based on SnO2/RGO Composites, *Front. Chem.*, **2021**, *9*, 681313.https://doi.org/10.3389/fchem.2021.681313.
179. Gomaa, M.M.; Sayed, M.H.; Patil, V.L.; Boshta, M.; Patil, P.S. Gas Sensing Performance of Sprayed NiO Thin Films toward NO2 Gas.*J. Alloys Compd.*, **2021**, *885*, 160908, https://doi.org/10.1016/j.jallcom.2021.160908.
180. Drewniak, S.; Drewniak, Ł.; Pustelny, T., Mechanisms of NO2 Detection in Hybrid Structures Containing Reduced Graphene Oxide: A Review. *Sensors*, **2022**, *22*, 5316, https://doi.org/10.3390/s22145316.
181. Huang, M.; Wang, Y.; Ying, S.; Wu, Z.; Liu, W.; Chen, D.; Peng, C., Synthesis of Cu2O-Modified Reduced Graphene Oxide for NO2 Sensors.*Sensors*, **2021**, *21*, 1958, https://doi.org/10.3390/s21061958.
182. Steinhauer, S., Gas Sensors Based on Copper Oxide Nanomaterials: A Review.*Chemosensors*, **2021**, *9*, 51, https://doi.org/10.3390/chemosensors9030051.
183. Zhou, L.; Hu, Z.; Wang, P.; Gao, N.; Zhai, B.; Ouyang, M.; Zhang, G.; Chen, B.; Luo, J.; Jiang, S.; Li, H.-Y.; Liu, H., Enhanced NO2 Sensitivity of SnO2 SAW Gas Sensors by Facet Engineering.*Sens. Actuators B Chem.*, **2022**, *361*, 131735, https://doi.org/10.1016/j.snb.2022.131735.
184. S., K.G.; Kaur, M.; M., S.; Pathak, A.; Gadkari, S.C.; Debnath, A.K., Highly Sensitive NO2 Sensor Based on ZnO Nanostructured Thin Film Prepared by SILAR Technique.*Sens. Actuators B Chem.*, **2021**, *335*, 129678, https://doi.org/10.1016/j.snb.2021.129678.
185. Hassinen, J.; Kauppila, J.; Leiro, J.; Määttänen, A.; Ihalainen, P.; Peltonen, J.; Lukkari, J., Low-Cost Reduced Graphene Oxide-Based Conductometric Nitrogen Dioxide-Sensitive Sensor on Paper. *Anal. Bioanal. Chem.*, **2013**, *405*, 3611–3617, https://doi.org/10.1007/s00216-013-6805-5.
186. Kotbi, A.; Imran, M.; Kaja, K.; Rahaman, A.; Ressami, E.M.; Lejeune, M.; Lakssir, B.; Jouiad, M., Graphene and G-C3N4-Based Gas Sensors. *J. Nanotechnol.*, **2022**, *2022*, 1–20, https://doi.org/10.1155/2022/9671619.
187. Gutés, A.; Hsia, B.; Sussman, A.; Mickelson, W.; Zettl, A.; Carraro, C.; Maboudian, R., Graphene Decoration with Metal Nanoparticles: Towards Easy Integration for Sensing Applications.*Nanoscale*, **2012**, *4*, 438–440, https://doi.org/10.1039/C1NR11537E.
188. Rigi Jangjoo, M.; Berahman, M., Room-Temperature Nitrogen Dioxide Gas Sensor Based on Graphene Oxide Nanoribbons Decorated with MoS2 Nanospheres.*Appl. Phys. A*, **2022**, *128*, 523, https://doi.org/10.1007/s00339-022-05605-x.
189. Park, H.; Kim, W.; Lee, S.W.; Park, J.; Lee, G.; Yoon, D.S.; Lee, W.; Park, J., Flexible and Disposable Paper-Based Gas Sensor Using Reduced Graphene Oxide/Chitosan Composite.*J. Mater. Sci. Technol.*, **2022**, *101*, 165–172, https://doi.org/10.1016/j.jmst.2021.06.018.
190. Bielecki, Z.; Janucki, J.; Kawalec, A.; Mikołajczyk, J.; Pałka, N.; Pasternak, M.; Pustelny, T.; Stacewicz, T.; Wojtas, J. Sensors and Systems for the Detection of Explosive Devices - An Overview.*Metrol. Meas. Syst.*, **2012**, *19*, 3–28, https://doi.org/10.2478/v10178-012-0001-3.
191. Tyszkiewicz, C.; Karasiński, P.; Rogoziński, R., Sensitive Films for Optical Detection of Ammonia and Nitrogen Dioxide.*Acta Phys. Pol. A*, **2012**, *122*, 915–920, https://doi.org/10.12693/APhysPolA.122.915.
192. Pustelny, T.; Procek, M.; Maciak, E.; Stolarczyk, A.; Drewniak, S.; Urbańczyk, M.; Setkiewicz, M.; Gut, K.; Opilski, Z. Gas Sensors Based on Nanostructures of Semiconductors ZnO and TiO2, *Bull. Pol. Acad. Sci. Tech. Sci.***2012**, *60*, 853–859, https://doi.org/10.2478/v10175-012-0099-1.
193. Hill, E.W.; Vijayaragahvan, A.; Novoselov, K., Graphene Sensors.*IEEE Sens. J.*, **2011**, *11*, 3161–3170, https://doi.org/10.1109/JSEN.2011.2167608.
194. Kaniyoor, A.; Imran Jafri, R.; Arockiadoss, T.; Ramaprabhu, S., Nanostructured Pt Decorated Graphene and Multi Walled Carbon Nanotube Based Room Temperature Hydrogen Gas Sensor.*Nanoscale*, **2009**, *1*, 382, https://doi.org/10.1039/b9nr00015a.
195. Pustelny, T.; Setkiewicz, M.; Drewniak, S.; Maciak, E.; Stolarczyk, A.; Procek, M.; Urbańczyk, M.; Gut, K.; Opilski, Z.; Pasternak, I.; Strupinski, W., The Influence of Humidity on the Resistance Structures with

Graphene Sensor Layer.*Acta Phys. Pol. A*, **2012**, *122*, 870–873, https://doi.org/10.12693/APhysPolA.122.870.
196. Van Cat, V.; Dinh, N.X.; Ngoc Phan, V.; Le, A.T.; Nam, M.H.; Dinh Lam, V.; Dang, T.V.; Quy, N.V., Realization of Graphene Oxide Nanosheets as a Potential Mass-Type Gas Sensor for Detecting NO2, SO2, CO, and NH3.*Mater. Today Commun.*, **2020**, *25*, 101682, https://doi.org/10.1016/j.mtcomm.2020.101682.
197. Zhang, H.; Li, Q.; Huang, J.; Du, Y.; Ruan, S., Reduced Graphene Oxide/Au Nanocomposite for NO2 Sensing at Low Operating Temperature, *Sensors*, **2016**, *16*, 1152, https://doi.org/10.3390/s16071152.
198. Dhingra, V.; Kumar, S.; Kumar, R.; Garg, A.; Chowdhuri, A., Room Temperature SO 2 and H 2 Gas Sensing Using Hydrothermally Grown GO–ZnO Nanorod Composite Films, *Mater. Res. Express*, **2020**, *7*, 065012, https://doi.org/10.1088/2053-1591/ab9ae7.
199. Lu, X.; Song, X.; Gu, C.; Ren, H.; Sun, Y.; Huang, J., Freeze Drying-Assisted Synthesis of Pt@reduced Graphene Oxide Nanocomposites as Excellent Hydrogen Sensor. *J. Phys. Chem. Solids*, **2018**, *116*, 324–330, https://doi.org/10.1016/j.jpcs.2018.02.006.
200. Park, J.; Kim, J.; Kim, K.; Kim, S.-Y.; Cheong, W.H.; Park, K.; Song, J.H.; Namgoong, G.; Kim, J.J.; Heo, J.; Bien, F.; Park, J.-U., Wearable, Wireless Gas Sensors Using Highly Stretchable and Transparent Structures of Nanowires and Graphene.*Nanoscale*, **2016**, *8*, 10591–10597, https://doi.org/10.1039/C6NR01468B.
201. An, B.W.; Shin, J.H.; Kim, S.-Y.; Kim, J.; Ji, S.; Park, J.; Lee, Y.; Jang, J.; Park, Y.-G.; Cho, E.; Jo, S.; Park, J.-U., Smart Sensor Systems for Wearable Electronic Devices, *Polymers*, **2017**, *9*, 303, https://doi.org/10.3390/polym9080303.
202. Imamura, G.; Minami, K.; Shiba, K.; Mistry, K.; Musselman, K.; Yavuz, M.; Yoshikawa, G.; Saiki, K.; Obata, S., Graphene Oxide as a Sensing Material for Gas Detection Based on Nanomechanical Sensors in the Static Mode. *Chemosensors*, **2020**, *8*, 82, https://doi.org/10.3390/chemosensors8030082.
203. Bai, Y.; Xu, T.; Zhang, X., Graphene-Based Biosensors for Detection of Biomarkers. *Micromachines*, **2020**, *11*, 60, https://doi.org/10.3390/mi11010060.
204. Babu, K.; Rendén, G.; Afriyie Mensah, R.; Kim, N.K.; Jiang, L.; Xu, Q.; Restás, Á.; Esmaeely Neisiany, R.; Hedenqvist, M.S.; Försth, M.; Byström, A.; Das, O. A Review on the Flammability Properties of Carbon-Based Polymeric Composites: State-of-the-Art and Future Trends. *Polymers*, **2020**, *12*, 1518, https://doi.org/10.3390/polym12071518.
205. Georgakilas, V.; Otyepka, M.; Bourlinos, A.B.; Chandra, V.; Kim, N.; Kemp, K.C.; Hobza, P.; Zboril, R.; Kim, K.S., Functionalization of Graphene: Covalent and Non-Covalent Approaches, Derivatives and Applications. *Chem. Rev.*, **2012**, *112*, 6156–6214, https://doi.org/10.1021/cr3000412.
206. Li, D.; Zhang, W.; Yu, X.; Wang, Z.; Su, Z.; Wei, G., When Biomolecules Meet Graphene: From Molecular Level Interactions to Material Design and Applications. *Nanoscale*, **2016**, *8*, 19491–19509, https://doi.org/10.1039/C6NR07249F.
207. Chauhan, N.; Maekawa, T.; Kumar, D.N.S., Graphene Based Biosensors—Accelerating Medical Diagnostics to New-Dimensions. *J. Mater. Res.*, **2017**, *32*, 2860–2882, https://doi.org/10.1557/jmr.2017.91.
208. Bhalla, N.; Jolly, P.; Formisano, N.; Estrela, P., Introduction to Biosensors. *Essays Biochem.*, **2016**, *60*, 1–8, https://doi.org/10.1042/EBC20150001.
209. Mannoor, M.S.; Tao, H.; Clayton, J.D.; Sengupta, A.; Kaplan, D.L.; Naik, R.R.; Verma, N.; Omenetto, F.G.; McAlpine, M.C., Graphene-Based Wireless Bacteria Detection on Tooth Enamel.*Nat. Commun.*, **2012**, *3*, 763, https://doi.org/10.1038/ncomms1767.
210. Koester, S.J., High Quality Factor Graphene Varactors for Wireless Sensing Applications.*Appl. Phys. Lett.*, **2011**, *99*, 163105, https://doi.org/10.1063/1.3651334.
211. Pumera, M., Graphene in Biosensing.*Mater. Today*, **2011**, *14*, 308–315, https://doi.org/10.1016/S1369-7021(11)70160-2.
212. Yildiz, G.; Bolton-Warberg, M.; Awaja, F., Graphene and Graphene Oxide for Bio-Sensing: General Properties and the Effects of Graphene Ripples.*Acta Biomater.*, **2021**, *131*, 62–79, https://doi.org/10.1016/j.actbio.2021.06.047.
213. Zhang, W.; Du, Y.; Wang, M.L., Noninvasive Glucose Monitoring Using Saliva Nano-Biosensor. *Sens. Bio-Sens. Res.*, **2015**, *4*, 23–29, https://doi.org/10.1016/j.sbsr.2015.02.002.
214. Mao, K.; Wu, D.; Li, Y.; Ma, H.; Ni, Z.; Yu, H.; Luo, C.; Wei, Q.; Du, B., Label-Free Electrochemical Immunosensor Based on Graphene/Methylene Blue Nanocomposite.*Anal. Biochem.*, **2012**, *422*, 22–27, https://doi.org/10.1016/j.ab.2011.12.047.
215. Yang, W.; Ratinac, K.R.; Ringer, S.P.; Thordarson, P.; Gooding, J.J.; Braet, F., Carbon Nanomaterials in Biosensors: Should You Use Nanotubes or Graphene?.*Angew. Chem. Int. Ed.*, **2010**, *49*, 2114–2138, https://doi.org/10.1002/anie.200903463.
216. Wang, C.; Cui, X.; Li, Y.; Li, H.; Huang, L.; Bi, J.; Luo, J.; Ma, L.Q.; Zhou, W.; Cao, Y.; Wang, B.; Miao, F., A Label-Free and Portable Graphene FET Aptasensor for Children Blood Lead Detection.*Sci. Rep.*, **2016**, *6*, 21711, https://doi.org/10.1038/srep21711.

217. Ng, S.P.; Qiu, G.; Ding, N.; Lu, X.; Wu, C.-M.L., Label-Free Detection of 3-Nitro-l-Tyrosine with Nickel-Doped Graphene Localized Surface Plasmon Resonance Biosensor.*Biosens. Bioelectron.*, **2017**, *89*, 468–476, https://doi.org/10.1016/j.bios.2016.04.017.
218. He, L.; Pagneux, Q.; Larroulet, I.; Serrano, A.Y.; Pesquera, A.; Zurutuza, A.; Mandler, D.; Boukherroub, R.; Szunerits, S., Label-Free Femtomolar Cancer Biomarker Detection in Human Serum Using Graphene-Coated Surface Plasmon Resonance Chips.*Biosens. Bioelectron.*, **2017**, *89*, 606–611, https://doi.org/10.1016/j.bios.2016.01.076.
219. Prabowo, B.A.; Alom, A.; Secario, M.K.; Masim, F.C.P.; Lai, H.-C.; Hatanaka, K.; Liu, K.-C., Graphene-Based Portable SPR Sensor for the Detection of Mycobacterium Tuberculosis DNA Strain.*Procedia Eng.*, **2016**, *168*, 541–545, https://doi.org/10.1016/j.proeng.2016.11.520.
220. Ouyang, L.; Zhang, Q.; Ma, G.; Zhu, L.; Wang, Y.; Chen, Z.; Wang, Y.; Zhao, L., New Dual-Spectroscopic Strategy for the Direct Detection of Aristolochic Acids in Blood and Tissue.*Anal. Chem.*, **2019**, *91*, 8154–8161, https://doi.org/10.1021/acs.analchem.9b00442.
221. Xiu, X.; Hou, L.; Yu, J.; Jiang, S.; Li, C.; Zhao, X.; Peng, Q.; Qiu, S.; Zhang, C.; Man, B.; Li, Z., Manipulating the Surface-Enhanced Raman Spectroscopy (SERS) Activity and Plasmon-Driven Catalytic Efficiency by the Control of Ag NP/Graphene Layers under Optical Excitation.*Nanophotonics*, **2021**, *10*, 1529–1540, https://doi.org/10.1515/nanoph-2020-0644.
222. Li, N.; Tang, T.; Li, J.; Luo, L.; Li, C.; Shen, J.; Yao, J., Highly Sensitive Biosensor with Graphene-MoS2 Heterostructure Based on Photonic Spin Hall Effect.*J. Magn. Magn. Mater.*, **2019**, *484*, 445–450, https://doi.org/10.1016/j.jmmm.2019.04.003.
223. Ja'afar, P.N.S.S.; Razali, N.M.; Zaidi, N.F.A.; Ahmad, F.; Omar, M.F.; Ismail, A.K.; Rosdi, N.; Yaacob, M.H.; Hamzah, A.; Kaidi, H.M.; Ambran, S. *Graphene Coated Optical Fiber Tip Sensor for Nitrate Sensing Application* In: Proceedings of the 2020 IEEE 8th International Conference on Photonics (ICP); IEEE: Kota Bharu, Malaysia, **2020**; pp. 3–4, https://doi.org/10.1109/ICP46580.2020.9206450.
224. Krishnan, S.K.; Singh, E.; Singh, P.; Meyyappan, M.; Nalwa, H.S., A Review on Graphene-Based Nanocomposites for Electrochemical and Fluorescent Biosensors.*RSC Adv.*, **2019**, *9*, 8778–8881, https://doi.org/10.1039/C8RA09577A.
225. Nawrot, W.; Drzozga, K.; Baluta, S.; Cabaj, J.; Malecha, K., A Fluorescent Biosensors for Detection Vital Body Fluids' Agents.*Sensors*, **2018**, *18*, 2357, https://doi.org/10.3390/s18082357.
226. Sadighbayan, D.; Hasanzadeh, M.; Ghafar-Zadeh, E., Biosensing Based on Field-Effect Transistors (FET): Recent Progress and Challenges.*TrAC Trends Anal. Chem.*, **2020**, *133*, 116067, https://doi.org/10.1016/j.trac.2020.116067.
227. Bagherzadeh-Nobari, S.; Kalantarinejad, R., Real-Time Label-Free Detection of DNA Hybridization Using a Functionalized Graphene Field Effect Transistor: A Theoretical Study.*J. Nanoparticle Res.*, **2021**, *23*, 185, https://doi.org/10.1007/s11051-021-05295-1.
228. Bathinapatla, A.; Kanchi, S.; Sabela, M.I.; Ling, Y.C.; Bisetty, K.; Inamuddin, Experimental and Computational Studies of a Laccase Immobilized ZnONPs/GO-Based Electrochemical Enzymatic Biosensor for the Detection of Sucralose in Food Samples.*Food Anal. Methods*, **2020**, *13*, 2014–2027, https://doi.org/10.1007/s12161-020-01824-1.